13

DIFFUSION IN SOLIDS

This chapter, in which the primary aim is to obtain solutions to Fick's laws of diffusion, is similar to Chapter 9 where we presented solutions to heat conduction problems. Therefore, much of the groundwork laid in Chapter 9 reappears in the following discussions. We begin by presenting some classical approaches used for determining diffusion coefficients in solids, and then consider some applied problems involving diffusion in solids as the rate-limiting step.

13.1 STEADY-STATE DIFFUSION EXPERIMENTS

As an example of the application of Fick's first law, consider an iron tube held in the isothermal part of a furnace. A carburizing gas is passed through the inside of the tube, and a gas of a different composition is passed over the outside. The carbon activity, thus has a gradient from the inside surface to the outside surface. Steady state is reached when the carbon concentration at each point in the tube wall no longer changes with time. By this time, the appropriate differential equation for steady-state diffusion through a cylinder can be derived from shell balances. If the diffusion coefficient of carbon in iron is a constant, independent of composition, then by analogy with Eq. (9.13),

$$\frac{1}{r}\frac{d}{dr}\left[r\frac{dC}{dr}\right] = 0. \tag{13.1}$$

The solution to this equation is given by its heat transfer analog from Eq. (7.51):

$$\frac{C - C_2}{C_1 - C_2} = \frac{\ln (r/r_2)}{\ln (r_1/r_2)}, \tag{13.2}$$

where r_1 and r_2 are the inside and outside radii of the tube, and C_1 and C_2 are the corresponding concentrations of carbon at these surfaces. Thus a plot of C versus ln r should be a straight line. However, for carbon diffusing in γ-iron, the slope of such a plot, as shown in Fig. 13.1, becomes smaller on passing from the low-carbon side to the high-carbon side. Therefore, the diffusion coefficient must be a function of composition, Eqs. (13.1) and (13.2) do not apply, and we must approach the problem somewhat differently.

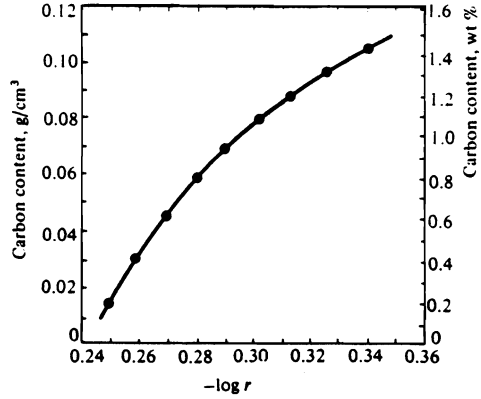

Fig. 13.1 Steady-state carbon concentration profile through a hollow cylinder of iron at 1000°C. (From R. P. Smith, *Acta Met.* **1**, 578 (1953).)

In addition to the fact that $\partial C/\partial t = 0$, steady state also means that the quantity of carbon passing through the tube per unit time is constant and independent of r. Thus

$$J = 2\pi r l j_r, \tag{13.3}$$

where l = length of the cylinder, j_r = local flux, and J = quantity of carbon passing through the tube wall per unit time. Since

$$j_r = -D\frac{dC}{dr}, \tag{13.4}$$

we may express Eq. (13.3) as

$$r\left[-D\frac{dC}{dr}\right] = \frac{J}{2\pi l},$$

or

$$\frac{dC}{d\ \ln r} = \frac{-J}{2\pi l D}. \tag{13.5}$$

For a given experiment, we can measure J and l, and if the carbon concentrations within the tube wall are determined by chemical analyses, then we can determine D from the slope of the plot of C versus ln r.

Similar experiments have also been performed for determining the diffusion coefficient of gases through metals such as, for example, the diffusion of hydrogen through a metal foil in Fig. 13.2. According to Fick's first law, the flux of hydrogen through the metal is

$$j_x = -D \frac{dC}{dx}. \tag{13.6}$$

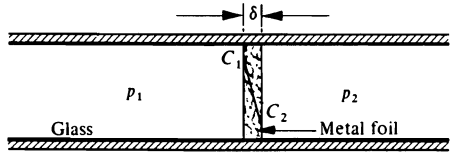

Fig. 13.2 Experiment for diffusion of hydrogen through metal foils.

The foils are very thin, and so it is extremely difficult to determine the concentration as a function of distance through the foil. The experimental results therefore consist of a measured steady-state flux, the hydrogen pressure drop across the foil, and the foil's thickness. To obtain D from the data, we take the value of C in the metal at each gas-metal interface as the solubility S that would exist in equilibrium with the gas.* From Sievert's law, we know that for equilibrium between gas and the metal

$$S_1 = Kp_1^{1/2}, \tag{13.7a}$$

and

$$S_2 = Kp_2^{1/2}, \tag{13.7b}$$

in which K is the equilibrium constant for the reaction

$$\tfrac{1}{2}H_2(g) = \underline{H} \text{ (in solution)}, \tag{13.8}$$

and p_1 and p_2 are the partial pressures of hydrogen on both sides of the foil with a thickness δ, as shown in Fig. 13.2.

The gradient dC/dx can then be expressed in terms of the pressures:

$$\frac{dC}{dx} = \frac{S_1 - S_2}{\delta} = \frac{K}{\delta}\left(\sqrt{p_1} - \sqrt{p_2}\right). \tag{13.9}$$

Combining Eqs. (13.6) and (13.9), we obtain the flux:

$$j_x = \frac{-DK}{\delta}\left(\sqrt{p_1} - \sqrt{p_2}\right). \tag{13.10}$$

*This is true under the conditions when the solution of gas in the surface of the metal occurs much more rapidly than the rate at which the diffusing species leaves the surface and enters the bulk metal. Experimentally, we check this assumption by determining the fluxes for two thicknesses of foil under the same pressure drop and temperature. If equilibrium does exist at the interface, then ΔC is the same for both cases, and the flux is inversely proportional to the thickness.

In relation to the diffusion of gases through solids, the term *permeability*, P, is often used and defined by

$$P = DS = DK\sqrt{p}\,, \tag{13.11}$$

so that

$$j_x = \frac{-(P_1 - P_2)}{\delta}, \tag{13.12}$$

and permeability is then given by an equation of the form

$$P = Ap^{1/2}e^{-Q_p/RT}, \tag{13.13}$$

which includes the temperature dependence of both S and D, with A and Q_p as constants. Unfortunately, there are also other ways to define permeability, which is rather confusing. For example, using a different definition, we obtain the flux:

$$j_x = -\frac{P^*}{\delta}\left(\sqrt{p_1} - \sqrt{p_2}\right), \tag{13.14}$$

so that $P^* = P = DS$ *only at 1 atm pressure, or 0.1013 MPa*:

$$P^* = DK. \tag{13.15}$$

In this case, we have

$$P^* = P_0^* e^{-Q_p/RT}. \tag{13.16}$$

The units given to P^* and P_0^* are not typically S.I. units; rather P_0^* = cm³(STP) s^{-1} cm^{-2} measured for 1 cm thickness and at 1 atm pressure, and Q_p = cal mol^{-1} (activation energy for permeation).

There are other sets of units which apply to P_0^* as well, and therefore one should be extremely careful of the term *permeability* because different definitions and units are used. Table 13.1 gives some representative data for various systems, using Eqs. (13.15) and (13.16) to define permeability. For data on permeability of gases through polymers, refer to Pauly.[1]

Table 13.1 Permeability data for gas-metal systems

Gas	Metal	P_0^*, cm³(STP) s^{-1} cm^{-1} atm$^{-1/2\dagger}$	Q_p, cal mol^{-1}
H_2	Ni	1.2×10^{-3}	13 850
H_2	Cu	$1.5\text{-}2.3 \times 10^{-4}$	16 000-18 700
H_2	α-Fe	2.9×10^{-3}	8400
H_2	Al	$3.3\text{-}4.2 \times 10^{-1}$	30 800
N_2	Fe	4.5×10^{-3}	23 800
O_2	Ag	2.9×10^{-3}	22 550

†The units in Eq. (13.14) are: δ = cm, p = atm, and j_x = cm³(STP) s^{-1} cm^{-2}.

[1]S. Pauly, "Permeability and Diffusion Data," in J. Brandrup and E. H. Immergut, editors, *Polymer Handbook*, third edition, John Wiley & Sons, New York, NY, 1989, pages VI/435 to VI/449.

Example 13.1 The solubility of hydrogen dissolved in aluminum at 873 K is 2.5×10^{-4} $cm^3(STP)\ g^{-1}$. Assume that Sievert's law holds. a) Calculate the equilibrium constant, b) the solubility in g cm^{-3}, and c) the diffusion coefficient for hydrogen in aluminum at 873 K.

Solution. a) When solubility data are given in this manner, it is assumed that the condensed phase has been equilibrated with the gas at 1 standard atm of pressure. Then, according to Eq. (13.8), the equilibrium constant is

$$K = \frac{S}{p^{1/2}}.$$

Therefore, K is simply

$$K = \frac{2.5 \times 10^{-4}\ cm^3(STP)}{1\ atm^{1/2}\ g} = 2.5 \times 10^{-4}\ cm^3(STP)\ atm^{-1/2}\ g^{-1}.$$

b) Notice the curious units for the *atomic* hydrogen dissolved in the aluminum (i.e., the solubility). The solubility is the mass of *molecular* hydrogen, expressed as a volume at standard temperature and pressure (STP). We did not invent these units, but they are the units most often given. Let's calculate a concentration in more familiar units. The density of Al at 873 K is 2.55 g cm^{-3}.

$$S = \frac{2.5 \times 10^{-4}\ cm^3(STP)}{g\ (Al)} \left| \frac{1\ mol\ (H_2)}{22\ 400\ cm^3(STP)} \right| \frac{2\ g\ (H)}{1\ mol\ (H_2)} \left| \frac{2.55\ g\ (Al)}{cm^3\ (Al)} \right.$$

$$= 5.69 \times 10^{-8}\ g\ cm^{-3}.$$

c) From Table 13.1, $P_0^* \simeq 0.37\ cm^3(STP)\ s^{-1}\ cm^{-1}\ atm^{-1/2}$ and $Q_p = 30\ 800\ cal\ mol^{-1}$. Then with Eq. (3.16) we calculate

$$P^* = 0.37 \exp\left[-\frac{30\ 800}{(1.987)(873)}\right] = 7.19 \times 10^{-9}\ cm^3(STP)\ s^{-1}\ cm^{-1}\ atm^{-1/2},$$

and

$$D = \frac{P^*}{K} = \frac{7.19 \times 10^{-9}\ cm^3(STP)}{s\ cm\ atm^{1/2}} \left| \frac{g(Al)\ atm^{1/2}}{2.5 \times 10^{-4}\ cm^3(STP)} \right| \frac{cm^3}{2.55\ g(Al)}$$

$$= 1.13 \times 10^{-5}\ cm^2\ s^{-1},$$

or $D = 1.13 \times 10^{-9}\ m^2\ s^{-1}$.

Example 13.2 A pilot plant for hydrogenation of hydrocarbon vapor is to be constructed of a low-alloy steel. In designing, the question of the effect of wall thickness on the rate of hydrogen loss through the wall is raised. If the inside diameter of a vessel 1 m long is 10 cm, calculate the rate of hydrogen loss as a function of wall thickness at 723 K and a pressure of 75 atm hydrogen, assuming that the gas diffusing through the wall is collected and removed at 1 atm.

Solution. Combining Eqs. (13.2), (13.3), and (13.4), and assuming that D is constant, we have

$$J = -2\pi lD \frac{C_1 - C_2}{\ln (r_1/r_2)}.$$

In terms of permeability

$$j = \frac{-2\pi lDK\left(\sqrt{p_1} - \sqrt{p_2}\right)}{\ln (r_1/r_2)} = \frac{-2\pi lP^*\left(\sqrt{p_1} - \sqrt{p_2}\right)}{\ln (r_1/r_2)}.$$

From Table 13.1 and Eq. (13.16), $P^* = 8.4 \times 10^{-6}$ cm^3(STP) s^{-1} cm^{-1} atm$^{-1/2}$. Therefore

$$J = \frac{-2\pi(100)(8.4 \times 10^{-6})\left(\sqrt{75} - \sqrt{1}\right)}{\ln r_1 - \ln r_2} = \frac{-0.0404}{1.609 - \ln r_2},$$

with the outside radius given in cm. In more general terms, where r_1 is not specified, but l is still 1 m,

$$J = \frac{-0.0404}{\ln (r_1/r_2)}, \text{ cm}^3\text{(STP) s}^{-1}.$$

Both results are shown below:

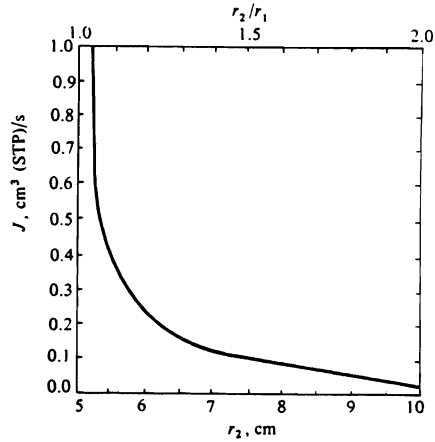

It probably makes sense to design the vessel with a 6 or 7 cm wall thickness.

13.2 TRANSIENT DIFFUSION EXPERIMENTS

Under many circumstances it is not possible to carry out steady-state experiments in order to determine diffusion coefficients in solids. This means that we must use the results of transient experiments and solve Eq. (12.18) in its general form

$$\frac{\partial C}{\partial t} = \nabla(D\nabla C) \tag{13.17}$$

for various boundary conditions. In correspondence with heat conduction, a solution to Eq. (13.17) is usually either a series of error functions, which converge rapidly for short times, or a trigonometric series which converges rapidly for long times. In the following sections, we examine several solutions to Eq. (13.17) and their applications.*

13.2.1 Thin film source: infinite and semi-infinite sink

The solution and procedure that follow have been used in self-diffusion studies of substitutional atoms. Radioactive tracers are used as solutes since their concentration can be determined quite accurately, even at low concentrations. A small quantity β of the tracer is plated as a thin film $\Delta x'$ thick on one end of a long rod of tracer-free material. The rod is then annealed at the diffusion temperature of interest. Since D^* is a self-diffusion coefficient and does not depend on position for such an application, Fick's second law is

$$\frac{\partial C}{\partial t} = D^* \frac{\partial^2 C}{\partial x^2}. \tag{13.18}$$

Suppose we take a second tracer-free rod and butt-weld it to the plated end (without any diffusion occurring), and then carry out the diffusion anneal. According to Eq. (9.45), we see that the solution is

$$C(x,t) = \frac{C_i}{2\sqrt{\pi D^* t}} \exp\left[\frac{-x^2}{4D^* t}\right] \Delta x'. \tag{13.19}$$

Here C_i is the concentration of the tracer in the plated material whose thickness is $\Delta x'$.

Since $C_i\,\Delta x'$ is the quantity of tracer material plated as the thin film, we write the solution

$$C(x,t) = \frac{\beta}{2\sqrt{\pi D^* t}} \exp\left[\frac{-x^2}{4D^* t}\right], \tag{13.20}$$

which describes the spreading by diffusion of a thin plate source into an infinite sink. This is illustrated in Fig. 13.3.

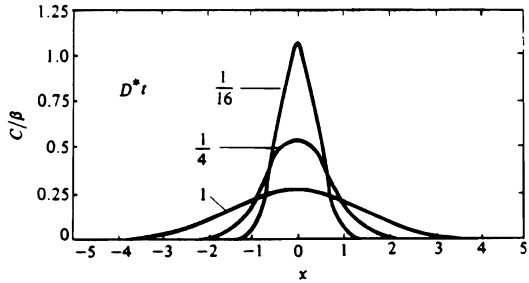

Fig. 13.3 Spreading of concentration from a plane source at $x = 0$.

*Extensive compilations of solutions are presented in J. Crank, *The Mathematics of Diffusion*, Oxford University Press, London, 1956, and W. Jost, *Diffusion in Solids, Liquids, and Gases*, Academic Press, 1960. With appropriate change of variables, one can also refer to H. S. Carslaw and J. C. Jaeger, *Conduction of Heat in Solids*, second edition, Oxford University Press, 1959.

Note that we may determine D^* without measurement or control of β, since a plot of log C versus x^2 at time t yields D^* directly.

Now suppose that the second bar has not been welded to the first. Then a *semi-infinite* bar would extend over the region $x > 0$ with an impermeable barrier at $x = 0$. In either case, infinite or semi-infinite,

$$\frac{\partial C}{\partial x} = 0 \qquad \text{at } x = 0. \tag{13.21}$$

If diffusion is allowed, the material that would normally diffuse in the negative x-direction is *reflected* at the $x = 0$ plane, and moves in the positive x-direction. The concentration at any x in the $+x$ domain is then given by the superposition of the original solution for $x > 0$ and the reflected solution for $x < 0$, or

$$C(x,t) = \frac{\beta}{\sqrt{\pi D^* t}} \exp\left[\frac{-x^2}{4D^* t}\right]. \tag{13.22}$$

13.2.2 Diffusion couple with constant $\widetilde{D}$

This case is exemplified in Fig. 13.4(a) by butt-welding two bars of *A-B* alloy of concentrations C_1 and C_2. If $\widetilde{D}$ is independent of composition, and the bars extend far enough in the positive and negative domains to be considered infinite, then Eq. (13.18) applies with the boundary conditions:

$$C(x,0) = C_1 \quad \text{at} \quad x < 0, \tag{13.23a}$$

$$C(x,0) = C_2 \quad \text{at} \quad x > 0, \tag{13.23b}$$

$$C(-\infty,t) = C_1, \tag{13.23c}$$

$$C(\infty,t) = C_2. \tag{13.23d}$$

Due to symmetry, the concentration at $x = 0$ immediately takes on the average value of C_1 and C_2. Let this average be C_s; then it is easy to see that in the positive x-domain, the solution is directly analogous to the temperature distribution of the semi-infinite solid, as discussed in Section 9.4.2 culminating in Eq. (9.62). Appropriately changing the symbols, we can write the solution:

$$\frac{C - C_s}{C_2 - C_s} = \text{erf}\,\frac{x}{2\sqrt{\widetilde{D}t}}. \tag{13.24}$$

Figure 13.4(b) illustrates this result in a general form, from which one may obtain $\widetilde{D}$-values from measurements of C, x, and t. Since erf x = –erf(–x), the concentration profile given by Eq. (13.24) is symmetrical about $x = 0$. This is known as the *Grube solution*, and applies when $\widetilde{D}$ is not a function of concentration. Since $\widetilde{D}$ is usually a function of composition, the use of Eq. (13.24) is restricted to small differences between C_1 and C_2. For example, a good value for the diffusion coefficient of A in 50*A*-50*B* alloy could be determined from a couple of 45% A alloy welded to a 55% A alloy.

Apart from application to diffusion couples, we can use Eq. (13.24) to predict concentration-time curves for situations where the part in which diffusion occurs is thick enough so that, within the time for diffusion, there is still a region of the part unchanged in composition.

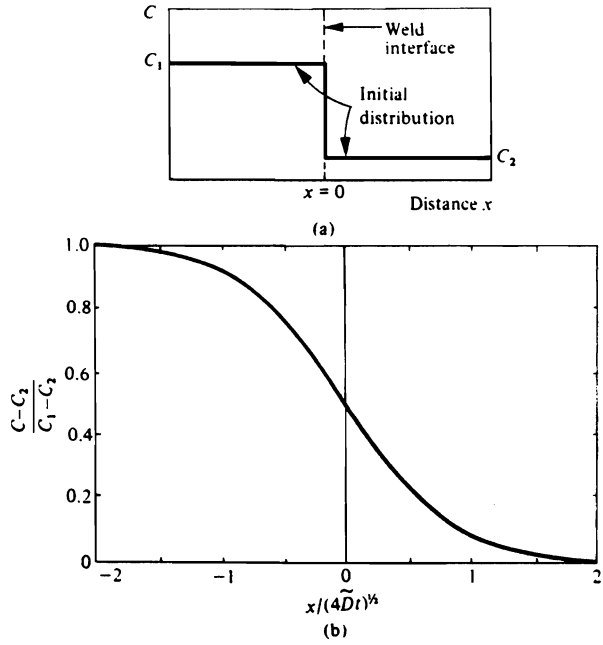

Fig. 13.4 Interdiffusion between an alloy of composition C_1 and an alloy of composition C_2. a) Initial distribution. b) Diffusion profile when the initial distribution is as in a).

Example 13.3 A piece of AISI 1020 steel is heated to 1255 K (in the austenite region) and subjected to a carburizing atmosphere such that the reaction

$$2CO = CO_2 + \underline{C}$$

is in equilibrium with 1.0% C in solution at the surface. Calculate the carbon profile after 1, 3, and 10 hours, assuming that diffusion within the solid is the rate-limiting step.

Solution. The initial condition is $C_2 = 0.2\%\ C$, and the boundary condition at the surface is $C_s = 1.0\%\ C$.

At 1255 K, $D_c = 2.0 \times 10^{-11}\ m^2\ s^{-1}$. Therefore, Eq. (13.24) for the distribution after 1 hour is

$$C(x,3600) = 1.0 + (0.2 - 1.0)\ erf\ \frac{x}{2\sqrt{(2 \times 10^{-11})(3.6 \times 10^3)}}.$$

Specifically at $x = 5 \times 10^{-4}$ m, $C = 0.35\%$ C. The results for various locations as well as for the longer times are:

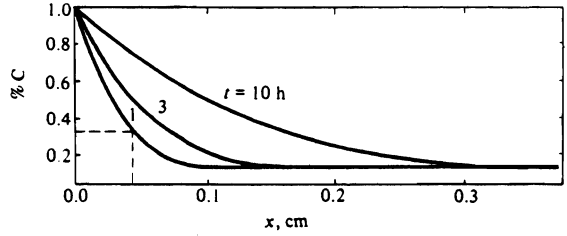

13.2.3 Diffusion couple with variable $\tilde{D}$

The analysis in Section 13.2.2 is valid only for $\tilde{D}$ independent of concentration. In general, however, the diffusion coefficient varies with composition, and since there is a concentration gradient, this means that $\tilde{D}$ changes with position. This variation in $\tilde{D}$ is particularly evident in diffusion couple experiments in which pure A is joined to pure B, and a continuous solid solution is formed. Fick's second law must be written over all compositions between A and B, and for such situations this is

$$\frac{\partial C}{\partial t} = \frac{\partial}{\partial x}\left[\tilde{D}\,\frac{\partial C}{\partial x}\right]. \tag{13.25}$$

The solution to Eq. (13.25) that follows is useful for obtaining $\tilde{D}$ over a range of compositions, but not for the *a priori* task of predicting a concentration profile for a diffusion anneal. In other words, it does not give a solution $C(x,t)$, which is usually sought, but rather allows $\tilde{D}(C)$ to be calculated from an experimental plot of $C(x)$. This method of analyzing experimental data is called the *Boltzmann-Matano* technique.

We combine the position variable x and the time variable t into one variable $\lambda = x/\sqrt{t}$, so that we consider C to be a function of only the one variable, λ. Using this definition of λ, we transform Eq. (13.25) into an ordinary differential equation:

$$\frac{\partial C}{\partial t} = \frac{\partial \lambda}{\partial t}\left[\frac{dC}{d\lambda}\right] = -\frac{1}{2}\,\frac{x}{t^{3/2}}\left[\frac{dC}{d\lambda}\right] = -\frac{\lambda}{2t}\left[\frac{dC}{d\lambda}\right], \tag{13.26a}$$

and

$$\frac{\partial C}{\partial x} = \frac{\partial \lambda}{\partial x}\left[\frac{dC}{d\lambda}\right] = \frac{1}{t^{1/2}}\left[\frac{dC}{d\lambda}\right]. \tag{13.26b}$$

Substituting into Eq. (13.25), we obtain

$$-\frac{\lambda}{2t}\left[\frac{dC}{d\lambda}\right] = \frac{\partial}{\partial x}\left[\frac{\tilde{D}}{t^{1/2}}\left[\frac{dC}{d\lambda}\right]\right] = \frac{1}{t}\,\frac{d}{d\lambda}\left[\tilde{D}\,\frac{dC}{d\lambda}\right],$$

or finally we can get

$$-\frac{\lambda}{2}\,\frac{dC}{d\lambda} = \frac{d}{d\lambda}\left[\tilde{D}\,\frac{dC}{d\lambda}\right]. \tag{13.27}$$

Consider the diffusion couple depicted in Fig. 13.5(a). Then for $C(\lambda)$, we recognize that

$$C = C_1, \quad \text{for } \lambda = -\infty, \tag{13.28a}$$

and

$$C = C_2, \quad \text{for } \lambda = +\infty. \tag{13.28b}$$

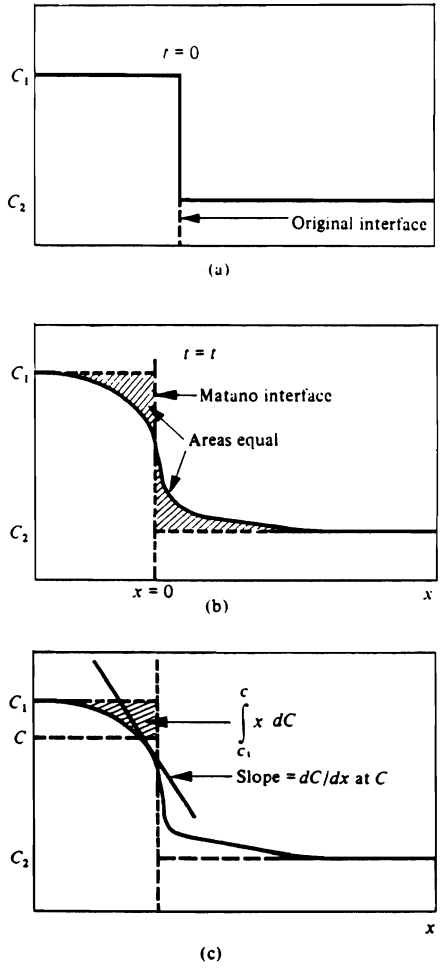

Fig. 13.5 a) Initial conditions. b) Definition of location of Matano interface after diffusion has taken place for a time t. c) The integral and the slope obtained in order to calculate $\tilde{D}$ at composition C.

We then solve Eq. (13.27) by integrating between $C = C_1$ and $C = C$:

$$-\tfrac{1}{2}\int_{C_1}^{C} \lambda dC = \widetilde{D}\left.\frac{dC}{d\lambda}\right|_{C_1}^{C}. \tag{13.29}$$

Since the concentration gradient goes to zero as C approaches C_1, the right-hand side of Eq. (13.29) is simply $\widetilde{D}(dC/d\lambda)$. Then

$$\widetilde{D} = -\frac{1}{2\left[\dfrac{dC}{d\lambda}\right]}\int_{C_1}^{C} \lambda dC. \tag{13.30}$$

From Eq. (13.29), we obtain the definition of the *Matano interface*; since the concentration gradient also goes to zero as C approaches C_2, Eq. (13.29) gives us the additional condition that

$$\int_{C_1}^{C_2} \lambda dC = 0. \tag{13.31}$$

Since experimental data are available only at some constant time t, Eqs. (13.30) and (13.31) can be written in terms of x and t, and the relationships used for calculating $\widetilde{D}$ from the measured concentration profile are

$$\widetilde{D} = -\frac{1}{2t}\frac{1}{\left[\dfrac{dC}{dx}\right]}\int_{C_1}^{C} x dC, \tag{13.32}$$

and we choose the plane defining $x = 0$ such that

$$\int_{C_1}^{C_2} x dC = 0. \tag{13.33}$$

In Fig. 13.5(b), the plane $x = 0$ is given by the line that makes the two hatched areas equal. We calculate the value of $\widetilde{D}$ at a given C by measuring the cross-hatched area, which is the integral in Eq. (13.32), and the reciprocal slope at that point, dx/dC. The diffusion coefficient $\widetilde{D}$, found by applying Eq. (13.32) in this manner, is the interdiffusion coefficient discussed in Section 13.2.3.

In addition, if we place inert markers at the original plane of welding, we can also determine the intrinsic diffusion coefficients. This is left for the reader to do in Problem 13.9. Furthermore, Jost[2] pointed out that it is not necessary for a single phase to exist over the entire range of the diffusion region. A discontinuity in $C(x)$ and $\widetilde{D}(C)$ exists where an intermediate phase is formed. The only condition required when applying the Boltzmann-Matano technique is that the concentrations in both phases on either side of the interface between the phases are independent of time.

---

[2]W. Jost, *Diffusion in Solids, Liquids, and Gases*, Academic Press, New York, 1960, page 76, and also W. Jost, *Z. Physik* **127**, 163 (1950).

Example 13.4 A diffusion couple made of pure Nb welded to pure U is held at 800°C for 49 days. The resulting concentration profile, shown below, is obtained with a microprobe analyzer. Note that an intermediate phase δ is formed between the two solid solution, γ_1 and γ_2. Calculate $\tilde{D}$ at 90 at.% U.

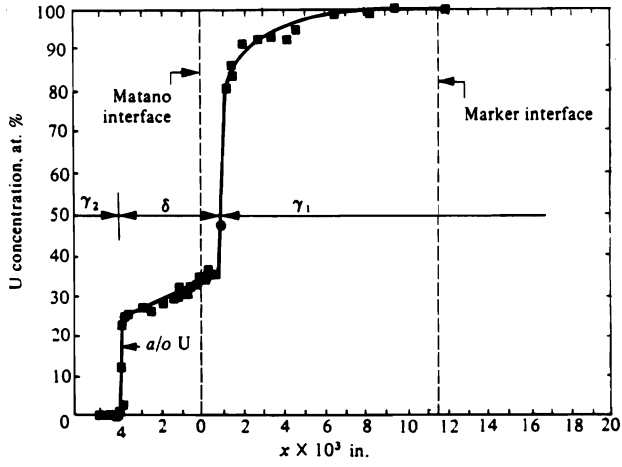

(From N. L. Peterson and R. F. Ogilvie, *Trans. AIME* **218**, 439 (1960).)

Solution. Let C represent the composition of U. First, the Matano interface is chosen, such that

$$\int_{-\infty}^{0} x dC = \int_{0}^{\infty} x dC.$$

This is found by trial and error, and placed on the figure as shown.

At 90% U, dC/dx is evaluated:

$$dC/dx = 4.60 \times 10^3 \text{ at.\% in}^{-1} = 1.81 \times 10^5 \text{ at.\% m}^{-1}.$$

Also

$$\int_{C=100}^{C=90} x dC = -1.32 \times 10^{-3} \text{ m at.\%, by graphical means;}$$

$$t = \frac{49 \text{ days} \mid 3600 \text{ s} \mid 24 \text{ h}}{\mid \text{h} \mid \text{day}} = 4.23 \times 10^6 \text{ s}.$$

Thus

$$\tilde{D} \text{ (90\% U)} = \frac{-(-1.32 \times 10^{-3})}{2(4.23 \times 10^6)(1.810 \times 10^5)} = 8.6 \times 10^{-16} \text{ m}^2 \text{ s}^{-1}.$$

13.3 FINITE SYSTEM SOLUTIONS

The solutions to Fick's laws presented thus far represent useful cases in many situations when the sink cannot be considered infinite or semi-infinite. On the other hand, there are many situations in which the effect of the diffusion process on the composition is felt at the furthest point in the material prior to the end of the diffusion treatment. This condition can arise quite often when small parts are exposed to a gaseous environment, and there is diffusion of the gas species into the part. Conversely, metal and ceramic parts must often be degassed. When dealing with these situations, it is usually safe to assume that the rate-limiting step of the overall mass transfer is the diffusion of the gas species into the solid. Hence, we seek solutions of Fick's second law with a surface concentration imposed at time zero and maintained constant.

To illustrate this case, consider the diffusion into or out of a slab of infinite length and thickness $2L$. Initially the slab has a uniform concentration C_i, and then its surfaces are raised or lowered to C_s and maintained constant. Hence, we are seeking a solution to Fick's second law with constant $\widetilde{D}$ (or simply D):

$$\frac{\partial C}{\partial t} = D \frac{\partial^2 C}{\partial x^2}. \tag{13.34}$$

The initial and boundary conditions of interest are

$$C(x,0) = C_i, \tag{13.35a}$$

and at the slab center,

$$\frac{\partial C}{dx}(0,t) = 0, \tag{13.35b}$$

and at the surface,

$$C(L,t) = C_s. \tag{13.35c}$$

The solution to this problem can be determined in the same manner as the solution of the heat conduction equation in Section 9.4.2. By separation of variables it has the form:

$$\theta = X(x)G(t),$$

where θ is $(C - C_s)$, and all the boundary conditions can be written in a homogeneous form. According to Eqs. (9.34) and (9.35), we see that

$$X = c_1 \cos \lambda x + c_2 \sin \lambda x, \tag{13.36}$$

and

$$G = \exp\left(-\lambda^2 Dt\right). \tag{13.37}$$

Boundary condition (13.35b) requires that $c_2 = 0$, and when we apply (13.35c) $c_1 \cos \lambda L = 0$ results. This is satisfied by $\lambda = (2n + 1)\pi/2L$, where n is any integer from 0 to ∞. Hence

$$\theta = \sum_{n=0}^{\infty} A_n \exp\left[\frac{-(2n + 1)^2\pi^2}{4} \frac{Dt}{L^2}\right] \cos\left[\frac{(2n + 1)\pi}{2} \frac{x}{L}\right], \tag{13.38}$$

where the A_ns are now the constants involved. The initial condition, $\theta(x,0) = \theta_i = C_i - C_s$, remains to be satisfied and when substituted into Eq. (13.38), it yields:

$$\theta_i = \sum_{n=1,\text{odd}}^{\infty} A_n \cos \frac{(2n + 1)\pi}{2} \frac{x}{L}. \tag{13.39}$$

If we apply Fourier's analysis to Eq. (13.39) as we demonstrated previously for Eq. (9.38), then we obtain

$$A_n = \frac{(-1)^n}{(2n + 1)} \frac{4}{\pi} \theta_i. \tag{13.40}$$

Thus the solution we seek is

$$\frac{\theta}{\theta_i} = \frac{C - C_s}{C_i - C_s} = \frac{4}{\pi} \sum_{n=0}^{\infty} \frac{(-1)^n}{2n + 1} \exp\left[\frac{-(2n + 1)^2\pi^2}{4} \frac{Dt}{L^2}\right] \cos \frac{(2n + 1)\pi}{2} \frac{x}{L}. \tag{13.41}$$

Equation (13.41) is useful for describing concentration profiles as a function of time. However, the total amount of material that diffuses into or out of the slab is often of more interest, particularly when this is the only measurable quantity. So, the average concentration $\bar{C}$ is required:

$$\bar{C} = \frac{1}{L} \int_0^L C \, dx. \tag{13.42}$$

Carrying out this operation, using Eq. (13.41) for C, we obtain the relative change in average composition for diffusion into a slab:

$$\frac{\bar{C} - C_s}{C_i - C_s} = \frac{8}{\pi^2} \sum_{n=0}^{\infty} \frac{1}{(2n + 1)^2} \exp\left[\frac{-(2n + 1)^2\pi^2}{4} \frac{Dt}{L^2}\right]. \tag{13.43}$$

This expression is good for diffusion into or out of a slab. If we take the first term in the series, then

$$\frac{\bar{C} - C_s}{C_i - C_s} = \frac{8}{\pi^2} \exp(-t/\tau), \tag{13.44}$$

where τ is the time constant for the diffusion process ($\tau = 4L^2/\pi^2 D$). It is apparent that a graph of log $\bar{\theta}$ versus (t/τ) is a straight line and that we can obtain D from the slope. We plot Eq. (13.43) in Fig. 13.6, along with diffusion into or out of cylinders and spheres (see Table 13.2). For long times ($Dt/L^2 > 0.05$), the first term of the series is sufficient, and a straight line relationship is obeyed.

For diffusion into or out of simple multidimensional shapes other than the infinite plate, infinite cylinder, or sphere, we handle the problem in the same manner as we treated heat transfer to or from these shapes in Section 9.5. We can combine product solutions to yield the solution for the shape of interest.

Table 13.2 The relative change in average composition for the basic shapes

Diffusion in a slab of semithickness, L

I.C.: $C(x,0) = C_i$,

B.C.: $C(L,t) = C_s$,

$$\frac{\partial C}{\partial x}(0,t) = 0.$$

Solution:

$$\frac{\bar{C} - C_s}{C_i - C_s} = \frac{8}{\pi^2} \sum_{n=0}^{\infty} \frac{1}{(2n+1)^2} \exp\left[\frac{-(2n+1)^2\pi^2}{4} \frac{Dt}{L^2}\right]. \tag{13.43}$$

Diffusion in solid circular cylinder of radius, R

I.C.: $C(r,0) = C_i$,

B.C.: $C(R,t) = C_s$,

$$\frac{\partial C}{\partial r}(0,t) = 0.$$

Solution:

$$\frac{\bar{C} - C_s}{C_i - C_s} = \sum_{n=1}^{\infty} \frac{4}{\xi_n^2} \exp\left[\frac{-\xi_n^2 Dt}{R^2}\right], \tag{13.45}$$

where $\xi_n = 2.405, 5.520, 8.654, 11.792, 14.931$, when $n = 1, 2, 3, 4, 5$, etc.*

Diffusion in spheres of radius, R

The same set of initial and boundary conditions as for the cylinder above:

$$\frac{\bar{C} - C_s}{C_i - C_s} = \frac{6}{\pi^2} \sum_{n=1}^{\infty} \frac{1}{n^2} \exp\left[\frac{-n^2\pi^2 Dt}{R^2}\right]. \tag{13.46}$$

*ξ_n are roots of the equation $J_0(x) = 0$, where $J_0(x)$ is the Bessel function of zero order.

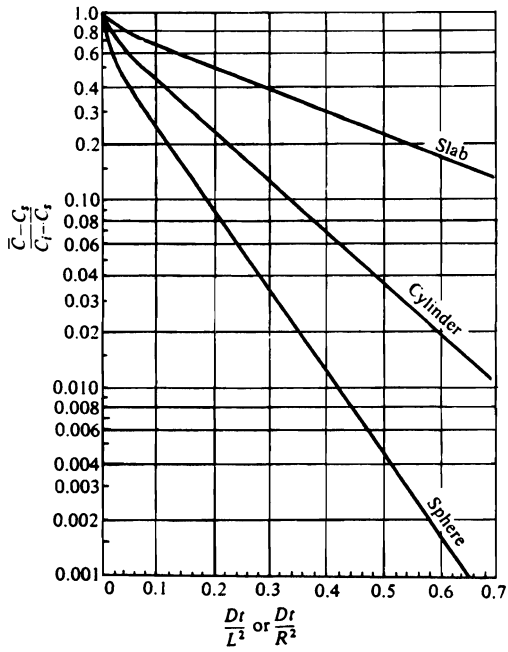

Fig. 13.6 The relative change in average composition for the basic shapes. R = radius, and L = semithickness.

Example 13.5 Calculate the fraction of hydrogen remaining in a) a 100 mm thick slab of steel, 3 m long × 1.2 m wide, b) a 100 mm square billet of steel, 4 m long, and c) a 100 mm square billet of steel, 200 mm long, after 40 hours of vacuum outgassing treatment at a temperature where $D_H = 1.0 \times 10^{-9}$ m^2 s^{-1}, assuming an initially uniform distribution.

Solution. a) Consider this to be an infinite plate. Then

$$\frac{Dt}{L^2} = \frac{(1 \times 10^{-9})(40 \times 3600)}{(5 \times 10^{-2})^2} = 5.76 \times 10^{-2}.$$

From Fig. 13.6, we have

$$\frac{\bar{C} - C_s}{C_i - C_s} = 0.74.$$

b) The desired solution can be obtained as the product of the infinite plate solutions for the two 100 mm dimensions:

$$\frac{\bar{C} - C_s}{C_i - C_s} = (0.74)(0.74) = 0.55.$$

c) In this case, first evaluate Dt/L^2 for the 200 mm dimension:

$$\frac{Dt}{L^2} = \frac{(1 \times 10^{-9})(40 \times 3600)}{0.1^2} = 1.44 \times 10^{-2}.$$

From Fig. 13.6, we get

$$\left[\frac{\bar{C} - C_s}{C_i - C_s}\right]_{200\ \text{mm}} = 0.90.$$

Therefore,

$$\frac{\bar{C} - C_s}{C_i - C_s} = (0.90)(0.74)(0.74) = 0.49.$$

13.4 MICROELECTRONIC DIFFUSION PROCESSING

Some materials result from processes in which alloying elements or *dopants* are diffused into a hot matrix to change electronic or magnetic properties. This is particularly true of silicon processed into devices. Frequently, a junction is fabricated by using two steps, each involving diffusion. The two steps are *predeposition* and *drive-in* diffusion.

In predeposition, a silicon wafer is placed in a high-temperature furnace and exposed to a gas that contains the dopant. Depending on the gas and the temperature, a constant concentration of the dopant is established at the surface. The goal of the predeposit step is to diffuse a small amount of the dopant into a fraction of a micrometer at the surface. Obviously, the silicon matrix is semi-infinite so the concentration profile of the dopant is

$$\frac{C - C_s}{C_0 - C_s} = \text{erf}\left[\frac{x}{2\sqrt{Dt}}\right], \tag{13.47}$$

where C_s is the constant surface concentration, C_0 is the initial concentration (assumed to be uniform), x is distance measured from the surface at $x = 0$, D is the diffusion coefficient of the dopant in the silicon, and t is time. The situation is depicted in Fig. 13.7.

The amount of dopant predeposited, usually expressed in terms of the number of dopant atoms, is

$$J = A \int_0^t j_{x=0}\, dt, \tag{13.48}$$

where A is the surface area of the silicon wafer and $j_{x=0}$ is the flux of dopant atoms at the surface ($x = 0$). It can be shown that the flux at the surface is

$$j_{x=0} = (C_s - C_0)\left[\frac{D}{\pi t}\right]^{1/2}; \tag{13.49}$$

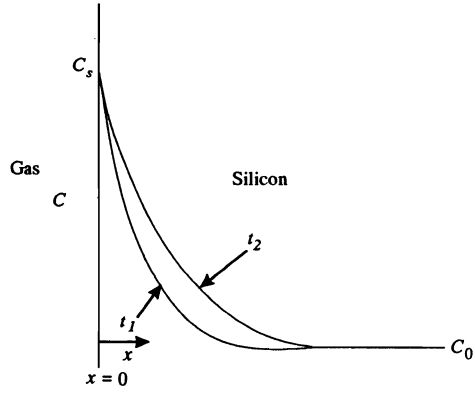

Fig. 13.7 The concentration of dopant at the surface of a silicon wafer during the predeposition step; $t_2 > t_1$.

then by combining Eqs. (13.48) and (13.49) and carrying out the integration, we get the amount predeposited. It is

$$J = \frac{2A}{\pi^{1/2}} (C_s - C_0)(Dt)^{1/2}. \tag{13.50}$$

During predeposition, we also calculate the diffusion depth of the dopant profile; it is

$$\ell = (Dt)^{1/2}. \tag{13.51}$$

Values of diffusion coefficients and approximate surface concentrations for two dopants, boron and phosphorus, are given in Table 13.3. The units are those most likely to be encountered in device fabrication technology.

Table 13.3 Surface concentrations and diffusion coefficients for boron and phosphorus

	Boron		Phosphorus	
T, K	C_s, atoms cm^{-3}	D, μm^2 h^{-1}	C_s, atoms cm^{-3}	D, μm^2 h^{-1}
1223	4.5×10^{20}	1.6×10^{-3}	9×10^{20}	1.7×10^{-3}
1273	4.8×10^{20}	5.2×10^{-3}	1.0×10^{21}	6.4×10^{-3}
1323	5.0×10^{20}	1.7×10^{-2}	1.1×10^{21}	2.0×10^{-2}
1373	5.1×10^{20}	5.8×10^{-2}	1.2×10^{21}	7.3×10^{-2}
1423	5.2×10^{20}	1.6×10^{-1}	1.2×10^{21}	1.8×10^{-1}

Example 13.6 Boron is predeposited on a silicon wafer with an initial concentration of 5×10^{15} atoms cm^{-3}. Conditions are 30 minutes at 1223 K. Calculate a) the amount deposited; b) the diffusion length; c) the concentration at the diffusion length.

Solution. a) From Table 13.3, $C_s = 4.5 \times 10^{20}$ atoms cm^{-3} and $D = 1.6 \times 10^{-3}$ μm^2 h^{-1}. Equation (13.50) applies, so that

$$\frac{J}{A} = \frac{2}{\pi^{1/2}}(C_s - C_0)(Dt)^{1/2} = \frac{2}{\pi^{1/2}}(4.5 \times 10^{20} - 5 \times 10^{15})(1.6 \times 10^{-3})^{1/2}(0.5)^{1/2}$$

$$= \frac{1.44 \times 10^{19} \text{ atoms } \mu\text{m}}{\text{cm}^3} \left| \frac{1 \text{ cm}}{10^4 \ \mu\text{m}} \right. = 1.44 \times 10^{15} \text{ atoms cm}^{-2}.$$

b) Equation (13.51) is used.

$$\ell = (1.6 \times 10^{-3} \times 0.5)^{1/2} = 2.83 \times 10^{-2} \ \mu\text{m} = 2.83 \times 10^{-6} \text{ cm}.$$

Notice how small ℓ is; this is typical.

c) Equation (13.47) applies with $x = \ell = (Dt)^{1/2}$. Thus, with Table 9.3 we get

$$\frac{C - C_s}{C_0 - C_s} = \text{erf}\left[\frac{1}{2}\right] = 0.5205,$$

and

$$C = (0.5205)(5 \times 10^{15} - 4.5 \times 10^{20}) + 4.5 \times 10^{20}$$

$$= 2.16 \times 10^{20} \text{ atoms cm}^{-3}.$$

From the above example we see that a very thin layer of the dopant is deposited on to the surface of the silicon matrix. This was done by the chemical reaction with the gas and allowing a small amount of diffusion to occur. Another method of producing a high concentration of dopant at the surface is *ion implantation*. In this method a beam of ions is accelerated into a mass-separating magnetic field, which selects the dopant ions from unwanted ions, similar to the separation in a mass spectrometer. The beam of dopant ions is aimed at the silicon target, where the ions come to rest after colliding with the nuclei and electrons in the surface layer of the target, which also tends to create vacancies in the host lattice. Ion implantation can be controlled better than predeposition through the gas, both in terms of minimizing lateral spread and in establishing a very sharp definition of the dopant at the surface. A very high density of crystalline defects, especially vacancies, however, is a disadvantage because they can reduce the electronic performance of the device.

After the predeposition step, drive-in diffusion is done to allow diffusion from the surface further into the silicon. This is illustrated by Fig. 13.8. To prevent escape of the dopant, a very thin layer of silica (SiO_2) is made on the surface. During the drive-in, the boundary conditions and the initial condition for $C(x,t)$ are

$$\frac{\partial C(0,t)}{\partial x} = 0, \tag{13.52a}$$

$$C(\infty,t) = C_0, \tag{13.52b}$$

and

$$C(x,0) = f(x'). \tag{13.52c}$$

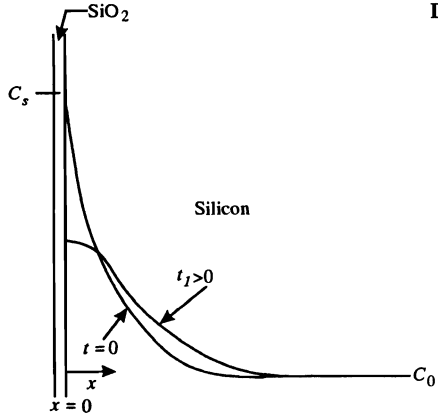

Fig. 13.8 The concentration of dopant near the surface of a silicon wafer during the drive-in step. The distribution at $t = 0$ is that from the predeposition step.

Equation (13.52a) applies at the surface, Eq. (13.52b) simply gives the concentration in the interior, and Eq. (13.52c) represents the distribution of dopant that results from the predeposition.

The solution which satisfies Fick's second law of diffusion and Eqs. (13.52a,b,c) can be deduced from Appendix G. Then

$$C - C_0 = \int_{x'=0}^{\infty} \frac{f(x') - C_0}{2\sqrt{\pi Dt}} \left\{ \exp\left[\frac{-(x - x')^2}{4Dt}\right] - \exp\left[\frac{-(x + x')^2}{4Dt}\right] \right\} dx', \quad (13.53)$$

where $f(x')$ is the distribution of the solute from the predeposition step and given by Eq. (13.47). By combining Eqs. (13.47) and (13.53), we get

$$\frac{C - C_0}{C_s - C_0} = \int_{x'=0}^{\infty} \frac{\operatorname{erfc}(x'/2\ell)}{2\sqrt{\pi Dt}} \left\{ \exp\left[\frac{-(x - x')^2}{4Dt}\right] - \exp\left[\frac{-(x + x')^2}{4Dt}\right] \right\} dx'. \quad (13.54)$$

Equation (13.54) is the solution, but, unfortunately, it is cumbersome and requires a numerical integration. Therefore, an approximate solution is often invoked.

The dopant taken up by the silicon in the predeposit step is approximated to be a thin source on the surface of the silicon. The strength of the source is given by the amount deposited per unit area. Thus, Eq. (13.22) applies with C relative to C_0 and the source strength (β) given by J/A, Eq. (13.50).

$$\frac{C - C_0}{C_s - C_0} = \frac{2}{\pi} \left[\frac{\ell^2}{Dt}\right]^{1/2} \exp\left[-\frac{x^2}{4Dt}\right]. \quad (13.55)$$

Notice that C_s and ℓ are from the predeposit step, but D and t are for the drive-in step.

The so-called "junction depth" (x_j) is important because it is a measure of the depth of diffusion after drive-in diffusion. The junction depth is defined as follows.

Since $C_s \gg C_0$, Eq. (13.55) is approximated by

$$\frac{C}{C_s} \cong \frac{2}{\pi} \left[\frac{\ell}{Dt}\right]^{1/2} \exp\left[-\frac{x^2}{4Dt}\right], \quad (13.56)$$

and x_j is that value of x where $C = C_0$. Then

$$x_j = \left\{ 4Dt \ln \left[\left(\frac{2}{\pi} \right) \left(\frac{C_s}{C_0} \right) \left(\frac{\ell^2}{Dt} \right)^{1/2} \right] \right\}^{1/2} \tag{13.57}$$

Example 13.7 After the predeposit step, the wafer of Example 13.6 is subjected to drive-in at 1423 K for 2 h. Calculate: a) the junction depth; b) the concentration at that depth; and c) the surface concentration.

Solution. a) Equation (13.57) applies with ℓ, C_s and C_0 given in Example 13.6. From Table 13.3 $D = 1.6 \times 10^{-1}\ \mu m^2\ h^{-1} = 4.44 \times 10^{-13}\ cm^2\ s^{-1}$; also $t = 7200$ s.

$$x_j = \left\{ 4 \times 4.44 \times 10^{-13} \right.$$

$$\left. \times\ 7200 \ln \left[\left(\frac{2}{\pi} \right) \left(\frac{4.5 \times 10^{20}}{5 \times 10^{15}} \right) \left(\frac{2.83^2 \times 10^{-12}}{4.44 \times 10^{-13} \times 7200} \right)^{1/2} \right] \right\}^{1/2}$$

$$x_j = 3.19 \times 10^{-4}\ cm = 3.19\ \mu m.$$

b) $C \simeq C_0 = 5 \times 10^{15}$ atoms cm^{-3}. We obtain an exact result by using Eq. (13.55).

$$\frac{C - C_0}{C_s - C_0} = \frac{2}{\pi} \left(\frac{2.83^2 \times 10^{-12}}{4.44 \times 10^{-13} \times 7200} \right)^{1/2} \exp \left(- \frac{3.19^2 \times 10^{-8}}{4 \times 4.44 \times 10^{-13} \times 7200} \right)$$

$$= 1.115 \times 10^{-5}.$$

Therefore,

$$C = (1.115 \times 10^{-5})(4.5 \times 10^{20} - 5 \times 10^{15}) + 5 \times 10^{15}$$

$$= 1.00 \times 10^{16}\ \text{atoms cm}^{-3}.$$

c) We use Eq. (13.55) with $x = 0$.

$$\frac{C - 5 \times 10^{15}}{4.5 \times 10^{20} - 5 \times 10^{15}} = \frac{2}{\pi} \left(\frac{2.83^2 \times 10^{-12}}{4.44 \times 10^{-13} \times 7200} \right)^{1/2} = 0.0319.$$

$$C = 1.43 \times 10^{19}\ \text{atoms cm}^{-3}.$$

13.5 HOMOGENIZATION OF ALLOYS

During solidification of alloys, *coring* occurs, because the rate of diffusion for most alloying elements in the solid state is too slow to maintain a solid of uniform concentration in equilibrium with the liquid. A cast structure is exemplified in Fig. 13.9 showing the repetitive pattern of microsegregation. In the case at hand we presume the alloy to be a single phase.

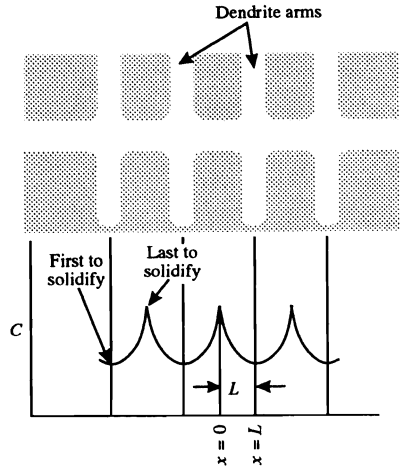

Fig. 13.9 A dendritic structure showing the *coring* or microsegregation of the alloying element. L is one-half of the dendrite arm spacing.

The dendrite arms develop during solidification and their spacing depends upon the alloy and the rate of cooling from the liquidus temperature to the nonequilibrium solidus temperature. Depending on the cooling rate, the *dendritic arm spacing* can be between 5 μm and 400 μm, with typical values ranging from 50 μm to 200 μm.

Dendritic structures occur in cast products that encompass ingots, shaped castings, continuous castings, and weldments. The coring, or microsegregation, is coincidental with the growth of the dendrites. Imagine a local region in a solidifying casting that comprises several to many dendrite arms. As solidification proceeds within the local region, solute is rejected to the *interdendritic* liquid, when the concentration of solute in the solid is less than that of the interdendritic liquid. The microsegregation can be closely approximated by a simple solute balance.[3] That is, the solute rejected from the dendritic solid equals the increase of solute in the interdendritic liquid. Therefore, within a local region undergoing solidification we have

$$(C_L - C_s^*)\,df_s = (1 - f_s)\,dC_L, \tag{13.58}$$

where

C_L = weight percent of solute in the interdendritic liquid;

C_s^* = weight percent of solute in the dendritic solid at the solid-liquid interface;

and

f_s = local weight fraction of solid.

---

[3]M. C. Flemings, *Solidification Processing*, McGraw-Hill, New York, NY, 1974, pages 34-36, 142.

When we use Eq. (13.58), it is assumed that there is sufficient diffusion of solute in the liquid so that it is uniform. This is usually valid because the diffusion length in the liquid is many times greater than the dendrite arm spacing. On the other hand, the diffusion coefficient of the solute in the solid is typically 5 or 6 orders of magnitude less than in the liquid, so we assume no diffusion in the solid. Consequently, as a layer of solid with a concentration C_s^* forms, its concentration never changes as subsequent solid of different C_s^* grows from the interdendritic liquid.

To get a quantitative picture of the microsegregation, we integrate Eq. (13.58). Then

$$\int_{C_L=C_0}^{C_L} \frac{dC_L}{C_L - C_s^*} = \int_{f_s=0}^{f_s} \frac{df_s}{1 - f_s},$$

or

$$1 - f_s = \exp\left[-\int_{C_L=C_0}^{C_L} (C_L - C_s^*)^{-1} dC_L\right], \tag{13.59}$$

where C_0 is the concentration of solute in the unsolidified melt (i.e., the alloy composition). In dendritically freezing alloys, the solid-liquid interface is very close to equilibrium so that C_s^* can be taken as the solid in equilibrium with the liquid. Many binary alloys have phase diagrams in which the ratio $C_s^*/C_L = k$ can be approximated as a constant, called the equilibrium partition ratio. With a constant k, we can substitute $C_s^* = kC_L$ into Eq. (13.59) and carry out the integration. The result is

$$\frac{C_L}{C_0} = (1 - f_s)^{k-1},$$

or

$$\frac{C_s^*}{C_0} = k(1 - f_s)^{k-1}. \tag{13.60}$$

As an example, suppose $k = 0.3$; then the microsegregation according to Eq. (13.60) is shown in Fig. 13.10. The first solid that forms has a concentration $C_s^* = kC_0$ and then succeeding solid has progressively higher values of C_s^*. But with no diffusion in the solid, the microsegregation, which develops, remains.

As $f_s \to 1$, Eq. (13.60) predicts $C_s^* \to \infty$. In reality, a reaction, such as a eutectic reaction, takes place near the end of solidification when the interdendritic liquid becomes sufficiently enriched in solute. In any event, after solidification is complete there is microsegregation, and in many applications it is necessary to subsequently heat treat the alloy to reduce the microsegregation by diffusion. This process is called homogenization.

During homogenization, the alloy naturally tends toward a uniform concentration (Fig. 13.11). We need only examine what happens within one dendritic element since the profile is periodic, and there is no net flow of solute from any dendritic region to the next.

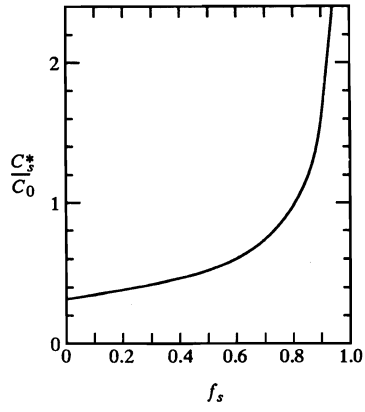

Fig. 13.10 Microsegregation in a dendritic solid with $k = 0.3$.

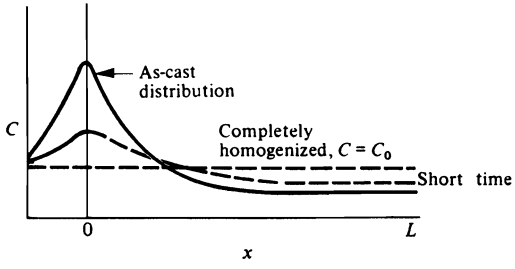

Fig. 13.11 Dendritic element, $0 < x < L$, used for describing homogenization kinetics.

To describe the homogenization kinetics, a solution to Fick's second law is needed that satisfies

$$\text{I.C.:}\quad C(x,0) = f(x), \tag{13.61a}$$

$$\text{B.C.:}\quad \frac{\partial C}{\partial x}(0,t) = 0, \tag{13.61b}$$

$$\frac{\partial C}{\partial x}(L,t) = 0, \qquad t > 0. \tag{13.61c}$$

The solution can be obtained by applying the method of separation of variables. Here we simply present the solution as given by Crank[4]:

$$C(x,t) = C_0 + \sum_{n=1}^{\infty} A_n \exp\left[-n^2\pi^2 \frac{Dt}{L^2}\right] \cos\frac{n\pi x}{L}, \tag{13.62}$$

[4]J. Crank, *The Mathematics of Diffusion*, Oxford University Press, London, 1957, page 58.

with

$$A_n = \frac{2}{L} \int_0^L f(x) \cos \frac{n\pi x}{L} \, dx. \tag{13.63}$$

In Eq. (13.62), C_0 is the overall or average alloy content, and we evaluate the A_ns by Eq. (13.63) using $f(x)$ as the initial solute distribution.

A useful parameter to describe the homogenization kinetics is the *residual segregation index* δ, which is defined as

$$\delta \equiv \frac{C_M - C_m}{C_M^0 - C_m^0}, \tag{13.64}$$

where C_M = maximum concentration, that is, $C_M = C(0,t)$; C_M^0 = initial maximum concentration, that is, $C_M^0 = C(0,0)$; C_m = minimum concentration, that is, $C_m = C(L,t)$; and C_m^0 = initial minimum concentration, that is, $C_m^0 = C(L,0)$. For no homogenization, $\delta = 1$, and after complete homogenization, $\delta = 0$.

We can find $C_M - C_m$ by applying Eq. (13.62) to $x = 0$ and $x = L$, and performing the indicated subtraction. The residual segregation index can then be written as

$$\delta = \frac{2 \sum_{n=1,3\ldots\text{odd}}^{\infty} A_n \exp\left[-n^2\pi^2 \frac{Dt}{L^2}\right]}{C_M^0 - C_m^0}. \tag{13.65}$$

Equation (13.65) has been used to analyze the homogenization of chromium in cast 52100 steel (1%C-1.5%Cr). Figure 13.12 shows the results. The practical conclusions of such studies show that:

1. In commercial material, with relatively large dendrite arm spacing (200-400 μm), substitutional elements do not homogenize unless excessively high temperatures and long diffusion times are employed. For example, in laboratory-cast 52100 ingots the dendrite arm spacing could typically be 300 μm, which would have to be held at 1450 K for about 20 hours to reduce δ to 0.2 for chromium. In large commercial ingots, dendrite arm spacings are larger and homogenization is even more difficult to achieve.
2. Significant homogenization of substitutional elements is possible at reasonable temperatures and times only if the material has fine dendrite arm spacings (<50 μm), which result from rapid solidification.
3. Interstitial elements (such as carbon in steel) diffuse very rapidly at austenizing temperatures.

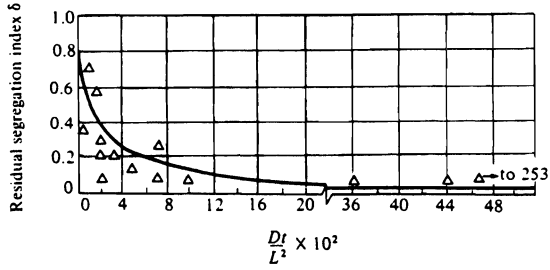

Fig. 13.12 The residual segregation index for chromium in cast 52100 steel. (From M. C. Flemings, D. R. Poirier, R. V. Barone, and H. D. Brody, *JISI*, 371, April 1970.)

Homogenization studies have also been carried out for 4340 low-alloy steel[5] and 7075 aluminum alloy.[6] In Reference 6, the analysis and discussion of homogenization emphasizes the dissolution of a nonequilibrium second phase during solutionizing.

Example 13.7 An ingot of 52100 steel goes through the processing schedule indicated below. Estimate the residual segregation index of chromium for the material in the center and the outside surface of the finished bar. Neglect the small amount of diffusion that occurs during blooming, rolling, and final cooling. Near the surface of the original cast ingot, the dendrite arm spacing is 40 μm, and in the center, it is 800 μm. The diffusion coefficient of chromium in this steel at these temperatures is given by

$$D = 2.35 \times 10^{-5} \exp [-17\,300/T(\mathrm{K})], \mathrm{cm}^2\ \mathrm{s}^{-1}.$$

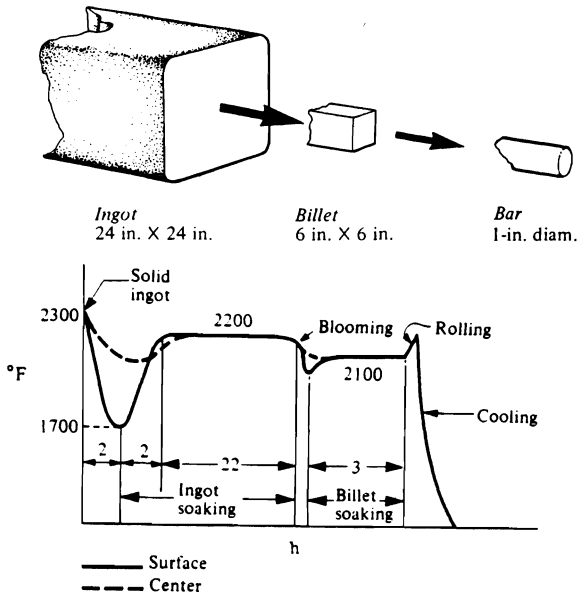

Reduction schedule for 52100 alloy steel bars.

Solution. Before proceeding directly to the solution of this problem, we should recognize that, although the basis for Eq. (13.65) assumes a constant diffusion coefficient (hence isothermal treatment), we can apply it to non-isothermal conditions.

For example, if a part is subjected to n heat treatment steps, each at a different temperature and for different times, we can compute the total magnitude of Dt/L^2 as

$$\frac{Dt}{L^2} = \frac{1}{L^2} \sum_{i=1}^{n} D_i t_i.$$

---

[5]T. F. Kattamis and M. C. Flemings, *Trans. TMS-AIME* **233**, 992 (1965).

[6]S. N. Singh and M. C. Flemings, *Trans. TMS-AIME* **245**, 1803 (1969).

We can then use this value of Dt/L^2 in Eq. (13.65). For a continuous nonisothermal situation, we compute the total magnitude of Dt/L^2 to be used as

$$\frac{Dt}{L^2} = \frac{1}{L^2} \int_0^t D(t)\, dt.$$

For hot-working in which D and L are both time dependent, Dt/L^2 should be evaluated as

$$\frac{Dt}{L^2} = \int_0^t \frac{D(t)}{[L(t)]^2}\, dt.$$

Now we determine $D(t)$, given the thermal process schedule and $D(T)$.

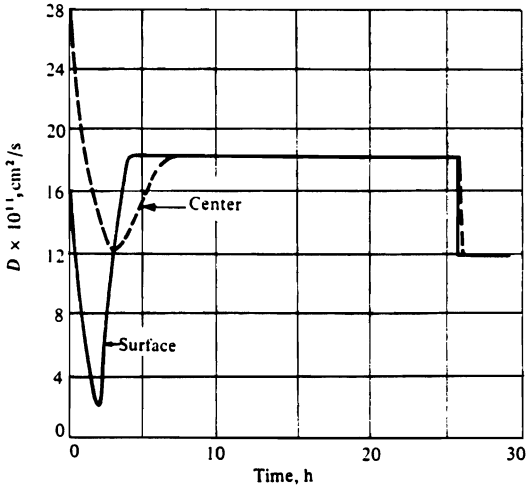

During the processing, assume that the dendrite spacing decreases in proportion to the changes of linear dimensions. Based on this, $L(t)$ is given in the table below.

Time	Center of ingot, L, cm	Surface of ingot L, cm
0-26 h	0.040	0.0020
26-29 h	0.010	0.0005

Now Dt/L^2 for the "surface" material can be evaluated by determining the area under the curve in the figure below.

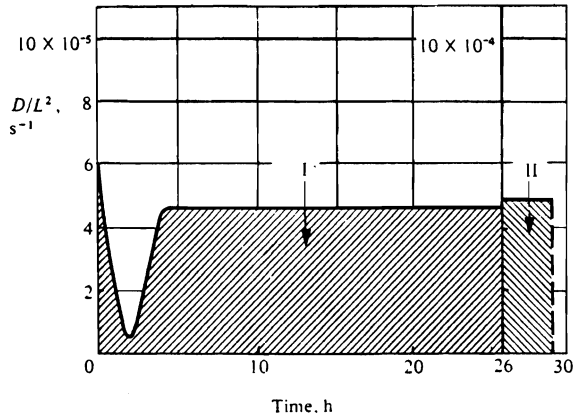

Under area I	112×10^{-5} h s^{-1}
Under area II	141×10^{-5} h s^{-1}
Total	253×10^{-5} h s^{-1}

$$\frac{Dt}{L^2} \text{ (surface)} = 253 \times 10^{-5} \times 3600 = 9.10.$$

According to Fig. 13.12, this value of Dt/L^2 indicates that the surface material would be homogeneous since $\delta \cong 0$.

In the center of the ingot, since the dendrite spacing is 20 times the spacing of the surface, then (neglecting small differences in the thermal history)

$$\frac{Dt}{L^2} \text{ (center)} \cong \frac{Dt}{L^2} \text{ (surface)} \times \frac{1}{20^2} = \frac{9.10}{400} = 0.0228.$$

From Fig. 13.12, we see that $\delta \cong 0.27$, and a significant amount of microsegregation remains in the material.

13.6 FORMATION OF SURFACE LAYERS

The rate of formation of oxide (sulfide) layers on metals and alloys exposed to oxidizing (sulfidizing) conditions is a matter of considerable technological importance. In general, it is not possible to say *a priori* that the rate of formation of a nonmetallic layer will be controlled by diffusion. For example, the initial rate of formation of the layer is often determined by the rate of an interface reaction between the gas and solid. As growth proceeds, if the specific volume of the oxide is much larger than that of the metal substrate, separation of the two phases may occur, causing an interruption in the growth of the oxide layer. However, in many cases this separation does not occur, and growth continues by diffusion of either the metal out through the oxide layer, or diffusion of oxygen into the metal-oxide interface, or a combination of both. In the case of adherent oxides, eventually

the diffusion flux slows down to the point where it is considerably slower than the interface reaction, and diffusion controls the rate of growth of the layer from then on.

If we consider the situation in Fig. 13.13, we can derive an expression for the rate of increase in the oxide thickness M. In this example, the metal is divalent, and the oxygen anions, having a large ionic radius, diffuse only at a negligible rate through the oxide layer so that $j_{O^{2-}} = 0$. Thus the oxide thickens because the metal cations diffuse through the oxide so that the oxidation reaction can proceed. At any instant, the flux of cations through the oxide is given by Fick's law (Eq. (12.2)):

$$j = (j_{A^{2+}}) = -D\left[\frac{\partial C}{\partial x}\right].$$

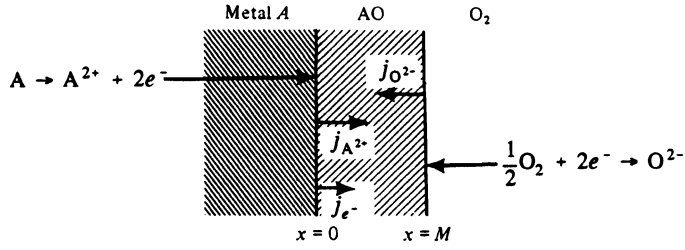

Fig. 13.13 The oxide layer on a metal showing the direction of flow of ions and electrons.

Here D is the diffusivity of the cation, and C is the cation concentration. If the oxide layer is thin, then we approximate the concentration profile of the cation as linear, and can integrate Fick's law as

$$j\int_0^M dx = -\int_{C_0}^{C_M} D\,dC.$$

Here, C_0 is the cation concentration at $x = 0$, and C_M is that at $x = M$. If the boundary conditions C_M and C_0 are unchanged with time (that is, with M), then the instantaneous flux *at any thickness* M is

$$j = \frac{1}{M}\int_{C_M}^{C_0} D\,dC, \tag{13.66}$$

or

$$j = \frac{k}{M},$$

where k is a constant, and has the units of mol m^{-1} s^{-1}.

The flux is proportional to the rate of growth of the thickness of the oxide layer:

$$j \propto \frac{dM}{dt},$$

or

$$\frac{k}{M} \propto \frac{dM}{dt}, \tag{13.67}$$

so that

$$\int_0^M M\, dM = \int_0^t k'\, dt,$$

or

$$M^2 = 2k't, \tag{13.68}$$

where k' is a constant with units $m^2\ s^{-1}$, known as the *Tammann scaling constant*[7] or the *Pilling and Bedworth constant*.[8] The parabolic nature of the rate of change of the oxide thickness with time is apparent.

Experimentally, it is usually more convenient to measure mass gain rather than the oxide thickness. Then

$$\frac{\Delta m}{A} = M\rho_0, \tag{13.69}$$

where $\Delta m/A$ = kg (mass gained) m^{-2} (surface area), and ρ_0 = concentration of oxygen in the oxide, kg of oxygen m^{-3} of oxide.

If we substitute Eq. (13.69) into Eq. (13.68), we obtain

$$\left[\frac{\Delta m}{A}\right]^2 = \frac{2k'}{\rho_0^2}\, t,$$

or

$$\left[\frac{\Delta m}{A}\right]^2 = k_p t, \tag{13.70}$$

where k_p is the *practical parabolic scaling constant*, $(\text{kg } O_2)^2\ m^{-4}\ s^{-1}$. Usually, we obtain experimental data by mass gain measurements, and take straight-line behavior when we plot $(\Delta m/A)^2$ versus t as an indication of diffusion-controlled oxidation.

Such data alone, however, do not indicate which *species* is responsible for the major material flow, that is, whether the metal is diffusing out from the oxide-metal interface or the oxygen is diffusing in. Wagner[9] has extended this simple expression to express k_p in terms of diffusion coefficients of the migrating species.

Combining Eqs. (12.23), (12.37), and (12.39), we obtain the relation

$$n_i B_i = \frac{t_i \sigma}{(z_i e)^2}, \tag{13.71}$$

---

[7]G. Tammann, *Z. Anorg. u. Allgem. Chem.* **111**, 78 (1920).

[8]N. B. Pilling and R. E. Bedworth, *J. Inst. Metals* **29**, 529 (1923).

[9]C. Wagner, *Atom Movements*, Amer. Soc. for Metals, Cleveland, OH, 1951, page 153.

where n_i = concentration of the migrating species, B_i = mobility of the species, σ = total electrical conductivity of the compound, t_i = transference number of species i, z_i = valence, and e = electronic charge. Now, using Eq. (12.32) and substituting Eqs. (12.37) and (13.71), we obtain the flux $\dot{n}_i$:

$$\dot{n}_i = -\frac{t_i\sigma}{(z_i e)^2}\left[\kappa_B T\left(\frac{\partial \ln n_i}{\partial x}\right) + z_i e\left(\frac{\partial \phi}{\partial x}\right)\right], \tag{13.72}$$

or in terms of the free energy for an ideal solution

$$\dot{n}_i = -\frac{t_i\sigma}{(z_i e)^2}\left[\frac{\partial \mu_i}{\partial x} + z_i e\,\frac{\partial \phi}{\partial x}\right], \tag{13.73}$$

where μ_i is the chemical potential (per atom) of species i. If the compound formed has the stoichiometric composition A_aB_b, where A is the cation, then the scale consists of ions according to the dissociation reaction:

$$A_aB_b = aA^{z_A+} + bB^{z_B-},$$

where the zs are the respective valences. Since the scale cannot have a net charge, the fluxes of individual species are related by

$$z_a\dot{n}_{A^+} = z_B\dot{n}_{B^-} + \dot{n}_e. \tag{13.74}$$

Using Eq. (13.73) for each flux and recalling Eq. (12.38), we obtain an expression for $\partial\phi/\partial x$:

$$\frac{\partial \phi}{\partial x} = \frac{1}{e}\left[-\frac{t_A}{z_A}\frac{\partial \mu_{A^+}}{\partial x} + \frac{t_B}{z_B}\frac{\partial \mu_{B^-}}{\partial x} + t_e\frac{\partial \mu_e}{\partial x}\right]. \tag{13.75}$$

In order to obtain an expression for the total flux in terms that we can measure, we must replace the expressions involving μ_{A^+}, μ_{B^-}, and μ_e. We first consider the equilibria

$$A = A^{z_A+} + z_A e, \tag{13.76a}$$

and

$$B + z_B e = B^{z_B-}. \tag{13.76b}$$

At equilibrium

$$\mu_A = \mu_{A^+} + z_A\mu_e, \tag{13.76c}$$

and

$$\mu_B = \mu_{B^-} - z_B\mu_e. \tag{13.76d}$$

For the compound in general, we get

$$d\mu_A = -\left|\frac{z_A}{z_B}\right| d\mu_B, \tag{13.77}$$

from the Gibbs-Duhem relationship. Then, eliminating μ_{A^+}, μ_{B^-}, and μ_e from Eqs. (13.75) and (13.73) and using Eqs. (13.76a,b) and (13.77), we obtain expressions for the particle fluxes:

$$\dot{n}_{A^+} = \frac{z_B t_A t_e \sigma}{z_A e^2 z_B^2} \left[\frac{\partial \mu_B}{\partial x}\right], \qquad A \text{ ions m}^{-2} \text{ s}^{-1} \tag{13.78}$$

and

$$\dot{n}_{B^-} = -\frac{t_B t_e \sigma}{e^2 z_B^2} \left[\frac{\partial \mu_B}{\partial x}\right], \qquad B \text{ ions m}^{-2} \text{ s}^{-1}. \tag{13.79}$$

Since the growth rate of the compound is the sum of the particle fluxes (although either may go to zero), we obtain

$$\dot{n}_{A_aB_b} = \frac{n_{A^+}}{a} - \frac{\dot{n}_{B^-}}{b} = \frac{\sigma(t_A + t_B)t_e}{e^2 z_B^2 b} \left[\frac{\partial \mu_B}{\partial x}\right], \qquad \text{molecules } A_aB_b \text{ m}^{-2} \text{ s}^{-1}. \tag{13.80}$$

If we use, for some reason, Eq. (13.80), we usually convert the units to give the flux in g-equivalents m^{-2} s^{-1}. Denoting the number of equivalents per mole by the symbol r,* we obtain the growth rate:

$$\dot{n}_{A_aB_b} = \frac{r\sigma(t_A + t_B)t_e}{e^2 z_B^2 N_0} \left[\frac{\partial \mu_B}{\partial x}\right], \qquad \text{g-equivalents } A_aB_b \text{ m}^{-2} \text{ s}^{-1}. \tag{13.81}$$

We define the *rational rate constant*, k_r, as $\int_0^x \dot{n}_{A_aB_b}\, dx$; then

$$k_r = \frac{r}{e^2 N_0 z_B^2} \int_{\mu_B^i}^{\mu_B^0} \sigma(t_A + t_B)t_e \, d\mu_B, \tag{13.82}$$

where μ_B^i and μ_B^0 are the chemical potentials of B at the inside and outside (metal and gas) interfaces of the oxide, respectively; k_r has the units of g-equivalents m^{-1} s^{-1} and is related to the parabolic rate constant k_p by

$$k_p = \frac{2\rho_0(\text{at. wt } B)^2}{r(\text{mol. wt } A_aB_b)} k_r. \tag{13.83}$$

The Tammann scaling constant is related to k_r by

$$k' = \frac{2(\text{at. wt } B)}{\rho_0 b z_B} k_r. \tag{13.84}$$

*Note that *numerically* $r = z_B$, but that their *units* differ.

If we assume that the anion exists as B_2 in the gaseous state, and there is ideal gas behavior, we can substitute

$$d\mu_B = \tfrac{1}{2}\kappa_B T\, d \ln p_{B_2}$$

into Eq. (13.82) and obtain

$$k_r = \frac{r\kappa_B T}{2e^2 N_0 z_B^2} \int_{p^i_{B_2}}^{p^O_{B_2}} t_e(t_A + t_B)\sigma \, d \ln p_{B_2}. \tag{13.85}$$

We note that although t_e may approach 1.0, and $(t_A + t_B)$ may approach zero, the expression $(t_A + t_B)$ cannot equal zero even for an electronic oxide conductor because it would cause a charge imbalance. In an electronic semiconductor, the product $t_e(t_A + t_B)$ is a very small number, and k_r is small. In this case, where $t_e = 1.0$, *if* we assume that *mobilities* B_A and B_B are equal to B_A^* and B_B^*, respectively, we can substitute Eq. (12.37) into Eq. (13.85) and obtain

$$k_r = \frac{n_B r}{2N_0} \int_{p^i_{B_2}}^{p^O_{B_2}} \left(\left| \frac{z_A}{z_B} \right|^2 \frac{n_A}{n_B} D_A^* + D_B^* \right) d \ln p_{B_2}. \tag{13.86}$$

When D_A^* or D_B^* are very different in magnitude, we may further simplify this expression as shown in the following example.

Example 13.8 Given the diffusion data for self-diffusion of Ni^{2+} and O^{2-} ions in NiO at 1190°C, calculate the rational rate constant and the parabolic rate constant for the oxidation of Ni in pure oxygen. It is known that $D_O^* \ll D_{Ni}^*$.

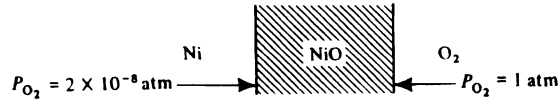

Solution. Since D_O^* is much less than D_{Ni}^*, we simplify Eq. (13.86) to

$$k_r = \frac{n_B r}{2N_0} \int_{p^i_{O_2}}^{p^O_{O_2}} D_{Ni}^* \, d \ln p_{O_2}.$$

The term $n_B r/N_0$ has the units of equivalents m^{-3}. In this case, we have

$$\frac{n_B r}{N_0} = \frac{2\rho_{NiO}}{\text{mol. wt}_{NiO}} = \frac{2(7.44 \times 10^3)}{74.69} = 1.99 \times 10^2 \text{ equivalents m}^{-3}.$$

Alternatively, if we take z_B as electronic charges per B atom, and n_B is the concentration of B atoms m^{-3}, then we must divide by Faraday's constant, 96 487 coulombs/equivalent, and multiply by the charge on an electron, 1.602×10^{-19} coulombs per charge. In this case, we get

$$k_r = \frac{n_B z_B e}{\mathscr{F} 2} \int_{p^i_{O_2}}^{p^O_{O_2}} D^*_{Ni}\ 2.3\ d \ln p_{O_2}$$

$$= \frac{(6.00 \times 10^{28})(2)(1.602 \times 10^{-19})}{2 \times 96\ 487} \int_{p^O_{B_2}}^{p^O_{B_2}} D^*_{Ni}\ d \ln p_{O_2}.$$

Thus either way

$$k_r = \frac{1.99 \times 10^2}{2} \int_{p^O_{B_2}}^{p^O_{B_2}} (D^*_{Ni})\ d \ln p_{O_2}.$$

We evaluate the integral graphically. The figure below gives D^*_{Ni} as a function of p_{O_2} in NiO. The area under the curve is equal to the integral/2.303. The area is

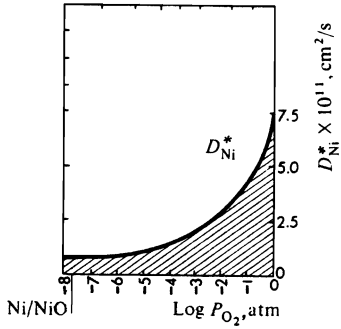

equal to 16×10^{-15} m^2 s^{-1}. Therefore

$$k_r = \left[\frac{1.99 \times 10^2}{2}\right](2.303)(16 \times 10^{-15}) = 3.66 \times 10^{-12} \text{ equivalents m}^{-1}\text{ s}^{-1}.$$

From Eq. (13.83), the parabolic rate constant is

$$k_p = \frac{2\rho_0(\text{mol. wt}_O)^2}{r(\text{mol. wt}_{NiO})} k_r = \frac{(2)(7.44 \times 10^3)(16^2)}{(2)(74.69)}(3.66 \times 10^{-12})$$

$$= 9.33 \times 10^{-8} (\text{kg O}_2)^2 \text{ m}^{-4} \text{ s}^{-1}.$$

Many metals exhibit parabolic oxidation kinetics, among them iron, nickel, cobalt, manganese, copper, and aluminum. Table 13.4 lists some typical values of k_p. Some, however, do not form compact, adherent oxides, and the kinetics of their oxidation are governed by either gas-solid reaction rates or gas-phase transport. For example, both molybdenum and tungsten form oxides that volatilize immediately upon reaction, and continually expose fresh metal to further oxidation, with no limit by solid-state diffusion on the rate.

Table 13.4 Parabolic oxidation constants for various metals

			Conditions	
Metal	Oxide	k_p, (kg O_2)^2 m^{-4} s^{-1}	Temp., °C	p_{O_2}, atm
Co	CoO	2.43×10^{-6}	1000	1.0
Cu	Cu_2O	6.3×10^{-7}	1000	0.083
Ni	NiO	3.8×10^{-8}	1000	1.0
Fe	FeO	1.6×10^{-5}	1000	3×10^{-14}
Fe	$FeO/Fe_3O_4/Fe_2O_3$	1.4×10^{-4}	1000	1.0
Ni-10%Cr	Complex	5.0×10^{-8}	1000	1.0
Cr	Cr_2O_3	1.3×10^{-9}	900	0.1
Fe-1%Ti	Complex	1.6×10^{-5}	1000	1.0
Al	Al_2O_3	8.5×10^{-14}*	600	1.0

*There is a considerable variation in this number, since the surface condition appears to have a strong effect.

Certain metals absorb a significant amount of oxygen in solid solution during the process of oxidation; zirconium, for example, can dissolve up to 29 at.% oxygen in solid solution prior to the formation of ZrO_2. Once the oxide layer has formed, its thickness increases in proportion to $\sqrt{k't}$, according to Eq. (13.79), and the thickness of the oxide as measured from the original surface is

$$M = \frac{2\hat{V}_{Zr}}{\hat{V}_{ZrO_2}} \sqrt{k't}\,, \tag{13.87}$$

where $\hat{V}_{Zr}$ is the molar volume of Zr and $\hat{V}_{ZrO_2}$ is the molar volume of ZrO_2. The diffusing species in the oxide is the oxygen anion moving in from the gas phase to the ZrO_2-Zr interface. At the interface, some of the oxygen dissolves in the metal, and some reacts to form more ZrO_2. Beyond the interface and into the metallic phase, for $x > M$, we have

$$\frac{\partial T}{\partial t} = D_O \frac{\partial^2 C}{\partial x^2}, \tag{13.88}$$

where C is the oxygen concentration, mol m^{-3}. If equilibrium is established at all times at the interface, and C_e is the oxygen content of the metal in equilibrium with ZrO_2, then

$$C(M,T) = C_e, \tag{13.89a}$$

$$C(\infty,t) = 0, \tag{13.89b}$$

$$C(x,0) = 0. \tag{13.89c}$$

The solution to Eq. (13.88) subject to Eqs. (13.87) and (13.89a,b,c) is

$$C = C_e \frac{\operatorname{erfc}\left[\dfrac{x}{2\sqrt{D_O t}}\right]}{\operatorname{erfc}\left[\dfrac{\hat{V}_{Zr}}{\hat{V}_{ZrO_2}}\sqrt{k'/D_O}\right]}, \tag{13.90}$$

where x is the distance from the original interface, and $x' = x - M$, where x' is the distance from the oxide-metal interface. Thus

$$C = C_e \frac{\operatorname{erfc}\left[\dfrac{x'}{2\sqrt{D_O t}} + \dfrac{\hat{V}_{Zr}}{\hat{V}_{ZrO_2}}\sqrt{k'/D_O}\right]}{\operatorname{erfc}\left[\dfrac{\hat{V}_{Zr}}{\hat{V}_{ZrO_2}}\sqrt{k'/D_O}\right]}. \tag{13.91}$$

PROBLEMS

13.1 One side of an iron sheet, 0.01 cm thick, is subjected to a carburizing atmosphere at 1200 K such that a surface concentration of 1.2% carbon is maintained. The opposite face is maintained at 0.1% carbon. At steady state, determine the flux (mol cm^{-2} s^{-1}) of carbon through the sheet: a) if the diffusion coefficient is assumed to be independent of concentration ($D = 2 \times 10^{-7}$ cm^2 s^{-1}); b) if the diffusion coefficient varies as shown to the right.

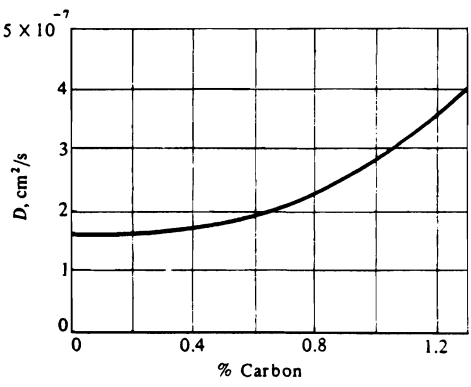

13.2 A composite foil made of metal A bonded to metal B, each 0.01 cm thick, is subjected to 0.5 atm of pure hydrogen on metal A's face; the other side, metal B's face, is subjected to a perfect vacuum. At the temperature of interest and 1 atm of hydrogen, the solubility of hydrogen in metal A is 4×10^{-4} g per cm^3 of A and in B it is 1×10^{-4} g per cm^3 of B. It is also known that hydrogen diffuses four times faster in A than B and that A and B do not diffuse in each other. Draw the concentration profile of hydrogen across the composite foil at steady state.

13.3 A thin sheet of iron at 800°C is subjected to different gaseous atmospheres on both of its surfaces such that the composition of one face is at 4 atom percent carbon and the other is at zero atom fraction carbon. At steady state, make a plot of the composition profile in the sample indicating *clearly* compositions and respective distances.

The thickness is 1 mm and density changes during the experiment may be neglected. At 800°C, it is known that the diffusion coefficient of carbon in iron is given by:

$$D = 10^{-6} \text{ cm}^2 \text{ s}^{-1} \text{ in ferrite } (\alpha),$$

$$D = 10^{-8} \text{ cm}^2 \text{ s}^{-1} \text{ in austenite } (\gamma).$$

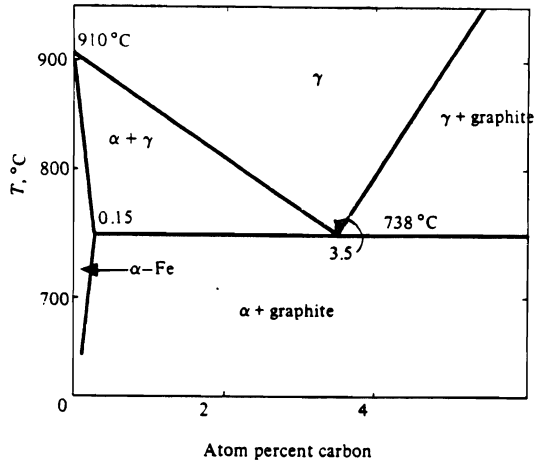

13.4 Often electronic packages are hermetically sealed with polymers, but after being put in service corrosion is sometimes observed. This happens because H_2O molecules can diffuse through polymers. Assume that the equilibrium between water vapor and water dissolved (or absorbed) by the polymer is simply represented by the reaction:

$$H_2O(g) = H_2O \text{ (dissolved)},$$

with the equilibrium constant

$$K = \frac{C}{p_{H_2O}} = 10^{-4}.$$

where C is the concentration of H_2O in the polymer (moles cm^{-3}) and p_{H_2O} is the pressure of $H_2O(g)$ in atm.

a) Assume equilibrium at the surfaces and calculate the flux of H_2O through the polymer (in moles cm^{-2} s^{-1}); assume steady state.

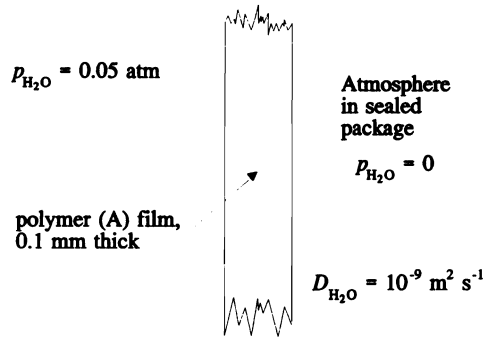

b) Now two films, polymer A and B, are used. Each is 0.1 mm thick.

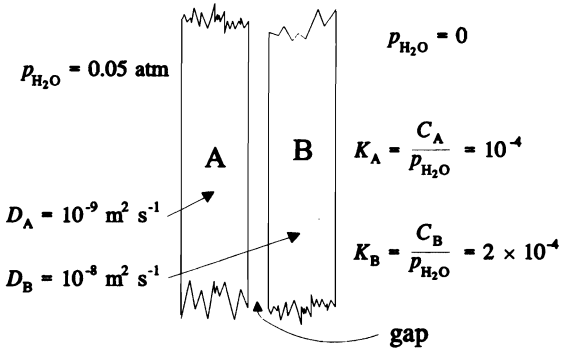

Assume steady state and equilibrium at all interfaces. What is the pressure of $H_2O(g)$ in the gap?

13.5 Hydrogen gas is maintained at 3 bar and 1 bar on opposite sides of a plastic membrane which is 0.3 mm thick. The temperature is 25°C, and the diffusion coefficient of hydrogen in the plastic is 8.7×10^{-10} m^2 s^{-1}. The solubility of hydrogen in the membrane is 1.5×10^{-3} kmol m^{-3} bar^{-1}. What is the mass diffusion flux of hydrogen through the membrane? Give your result in kmol s^{-1} m^{-2}.

13.6 The Grube solution is used to analyze diffusion data for a diffusion couple in which the solid is semi-infinite on both sides and when the chemical diffusion coefficient is uniform. Now consider a diffusion couple made from two thin solids so that the Grube solution for semi-infinite solids is not applicable. Such a couple is shown to the right with the initial condition for C_A shown. a) Assume that $\tilde{D}$ is uniform. Write a partial differential equation for $C_A(x,t)$ where x is the space coordinate and t is time. b) For $0 \leq x \leq L$, write appropriate boundary conditions and an appropriate initial condition for C_A. You may assume that component A is not volatile; i.e., no A is lost from the diffusion couple.

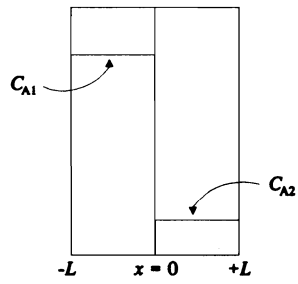

13.7 An unknown amount of radioactive gold is deposited as a thin layer on the ends of two rods of gold. The two rods are then joined to form a specimen having a planar source of radioactive gold (Au^*) atoms at the origin $x = 0$. After diffusion for 100 hours at 920°C, the distribution of Au^* is as shown below. Calculate the self-diffusion coefficient of gold in pure gold, based on the data at 0.3 mm and 0.6 mm as indicated in the plot of the relative concentration of gold.

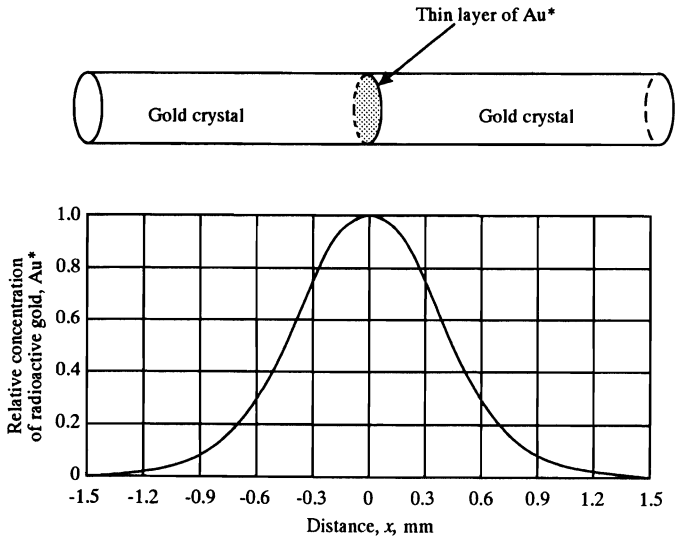

13.8 Silicon is exposed to a gas that establishes a concentration of 10^{18} atoms (Al) cm^{-3} on the surface of the silicon. The process is carried out at 1473 K. a) After 30 min, at what depth below the surface of the Si will the concentration be 10^{16} atoms cm^{-3}? b) Calculate the amount of Al (in atoms cm^{-2}) that diffuses into the Si after 30 min of treatment at 1473 K.

13.9 The Matano-Boltzmann analysis is used to calculate the interdiffusion coefficient, $\tilde{D}$, from diffusion couple data. It can also be used to determine the intrinsic diffusion coefficients in a binary by inserting inert markers at the original interface.

a) The distance moved by the markers is proportional to the square root of time. Show that v_x in Eq. (12.14) is given by

$$v_x = \frac{S}{2t},$$

where S is the distance moved by the markers and t is the diffusion time.

b) Assuming that $\tilde{D}$ and S are determined in a diffusion-couple, what two equations are needed to simultaneously solve for the intrinsic diffusion coefficients in the binary. [Hint: Review Section 12.2.2.]

13.10 A gold-nickel diffusion couple of limiting compositions $X_{Ni} = 0.0974$ and $X_{Ni} = 0.4978$ is heated at 925°C for 2.07×10^6 s. Layers 0.003 in. (0.0762 mm) thick and parallel to the original interface are machined off and analyzed. a) Using the data tabulated

below, calculate the diffusion coefficient at 20, 30, and 40 at.% nickel. b) Suppose that markers are inserted at the original interface and move along during the diffusion process at a composition of 0.30 atom fraction nickel. From this, determine the intrinsic coefficients of gold and nickel at 0.30 atom fraction nickel.

Slice No.	at% Ni	Slice No.	at% Ni	Slice No.	at% Ni	Slice No.	at% Ni
11	49.78	21	35.10	29	21.38	38	13.26
12	49.59	22	33.17	30	20.51	39	12.55
14	47.45	23	31.40	31	19.12	41	11.41
16	44.49	24	29.74	32	17.92	43	10.48
18	40.58	26	25.87	33	16.86	45	9.99
19	38.01	27	24.11	35	15.49	47	9.74
20	37.01	28	22.49	37	13.90		

13.11 Metals A and B form alloys of fcc structure at 1200°C. They are allowed to interdiffuse as a diffusion couple for 10^5 s, and the concentration profile obtained is given in the accompanying figure. Determine the value of the interdiffusion coefficient, $\tilde{D}$, at a concentration $C_B = 0.02$ mol cm^{-3}.

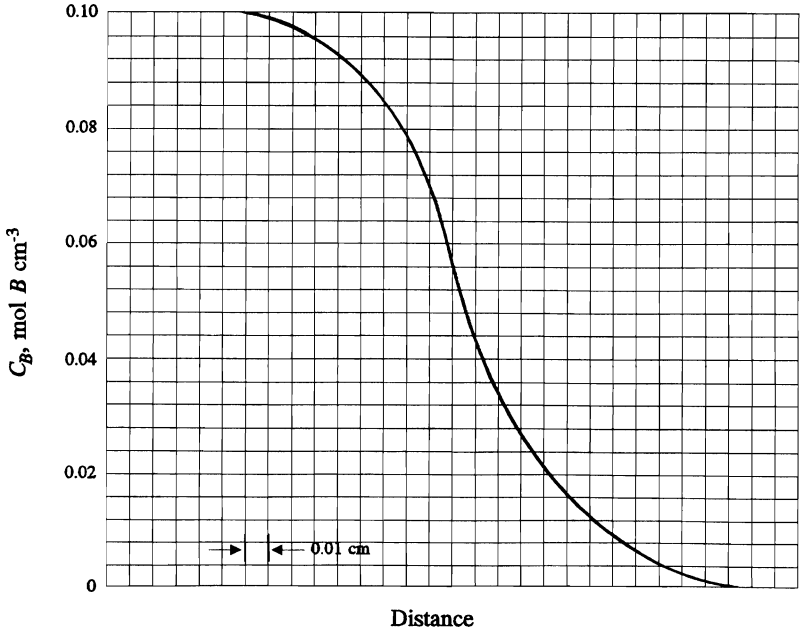

13.12 Intrinsic silicon (i.e., pure Si) is processed in a gas which establishes a concentration of 10 ppm (1 ppm = 10^{-4} wt.%) of boron at the surface of the silicon. Distances from the left vertical face are given in the following table.

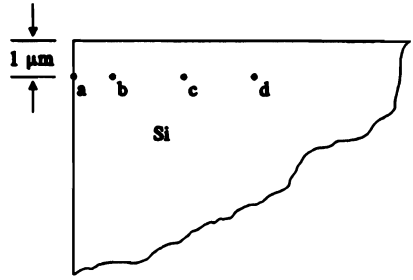

Point	Distance, μm
a	0
b	1
c	3
d	5

After 10 h exposure to the gas, what are the concentrations of boron at points a, b, c and d? At the process temperature, the diffusion coefficient for B in Si is $D = 10^{-12}$ cm^2 s^{-1} = 10^{-4} μm^2 s^{-1}.

13.13 A fine steel wire of 0.2 wt.% C is passed through a tube furnace at 1200°C which contains a carburizing gas. The composition of the carburizing gas is adjusted so that it fixes 0.8 wt.% C on the surface of the wire. By neglecting diffusion in the axial direction of the wire, calculate the average composition of the wire after it passes through the tube. At this temperature the steel is a single phase (austenite). *Data*: diameter of wire, 0.01 cm; length of furnace, L, 1.5 m; velocity of wire, V, 15 cm s^{-1}.

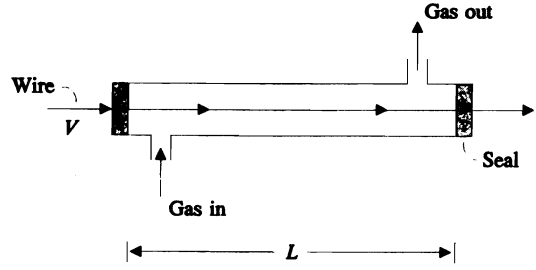

13.14 A thin layer of Au is plated on to the end of a Ni bar. The bar is annealed at 900°C for 10 h; at 900°C the interdiffusion coefficient of Au in Ni is 10^{-11} cm^2 s^{-1}. It is known that Au and Ni are completely soluble at 900°C. After the treatment, the concentration of Au at a distance of 0.05 cm from the end is 0.1 atom fraction of Au. At what distance from the end is the atom fraction of Au equal to 0.05?

13.15 A long cylindrical bar of steel which contains 3 ppm of hydrogen is dehydrogenated by a two-step vacuum process. The first step is treatment at 150°C for time period t_1, followed by the second step at 300°C for time period t_2. If $t_1 = 2t_2$, calculate: a) the total time ($t = t_1 + t_2$) to reduce the average composition to 1.5 ppm of hydrogen, and b) the center composition after the two-step treatment. *Data*: $D_H = 1.0 \exp(-4000/T)$ with D_H in cm^2 s^{-1} and T in K. The diameter of the bar is 2 cm.

13.16 The solubility of hydrogen in solid copper at 1000°C is 1.4 ppm (by mass) under a pressure of hydrogen of 1 atm. At 1000°C, $D_H = 10^{-6}$ cm^2 s^{-1}. a) Determine the time for hydrogen to reach a concentration of 1.0 ppm at a depth of 0.1 mm in a large chunk of copper initially with null hydrogen if the copper is subjected to 2 atm pressure of H_2 at

1000°C. b) Copper foil, 0.2 mm thick, is equilibrated with hydrogen at a pressure of 4 atm at 1000°C. The same foil is then placed in a perfect vacuum at 1000°C and held for 60 s. Calculate the concentration of hydrogen at the center of the foil after the 60 s period.

13.17 The term "banding" is used to describe chemical heterogeneity in rolled alloys that shows up as closely spaced light and dark bands in the microstructure of steel. These bands represent areas of segregation of alloying elements that formed during freezing of the ingot. During rolling the segregated areas are elongated and compressed into narrow bands. Assume that the alloy concentration varies sinusoidally with distance after rolling according to the sketch below.

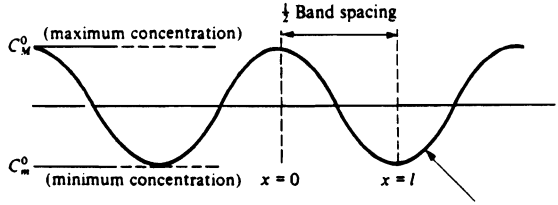

$$C = C_0 + (C_M^0 - C_0)\cos\frac{\pi x}{l}$$

If the steel is now heated to the austenite range and held at some constant temperature, then a) schematically sketch the concentration profile as time passes; b) write a differential equation for concentration (state assumptions) and c) write the boundary conditions (for time and space) that apply; d) solve for the concentration as a function of time and x; e) derive an equation for the residual segregation index.

13.18 Assume that the banding in a wrought cupronickel alloy (single phase) is described by the cosine function in Problem 13.17. The average composition of the alloy is 10% Ni-90% Cu, and the segregation ratio before homogenization is 1.4. Segregation ratio is defined as $S = C_M^0/C_m^0$. a) What are the maximum and minimum compositions of nickel? b) In order to homogenize the alloy in the shortest time possible, what temperature would you select? c) If the average distance between maximum compositions is 10^{-2} cm, determine the time to achieve a residual segregation ratio of 0.1 at 950°C. A diffusion coefficient can be obtained from Fig. 12.9. d) The alloy is given a "step" homogenization treatment which consists of 10 hours at 700°C, 10 hours at 800°C and 10 hours at 900°C. What is the residual segregation index after this treatment?

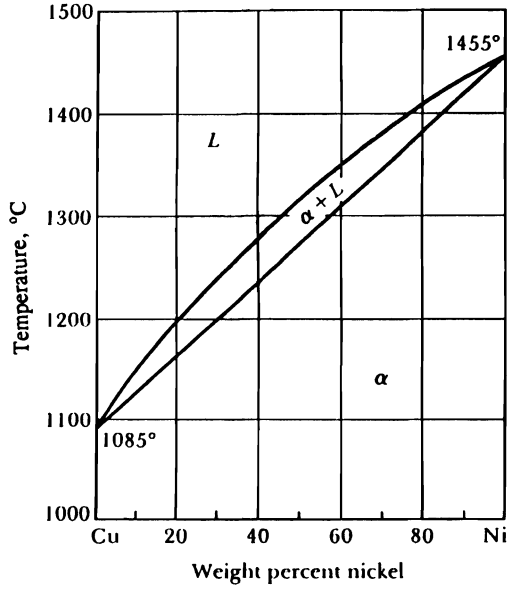

13.19 A junction in silicon is made by doping with boron using predeposition followed by drive-in diffusion. a) Five minutes at 1100°C are required to deposit the dopant. At what distance from the surface is the concentration of boron raised to 3×10^{18} atoms cm^{-3}. Assume that the silicon is initially pure. b) How much boron (per cm^2 of silicon surface) will have been taken up by the silicon during the deposition step? c) To prevent loss of boron during the drive-in step, the surface is masked with silica (SiO_2). Now calculate the time required to achieve a concentration of boron equal to 3×10^{18} atoms cm^3 at a depth of 6×10^{-4} cm if the drive-in treatment is carried out at 1150°C.

13.20 By ion implantation, lithium can be concentrated in a very thin surface layer (10^{-6} cm) on a nickel substrate. After implanting the surface layer, it has a lithium concentration of 10^{20} atoms cm^{-3}. Determine the time at 1000 K for reducing the surface concentration to 10^{19} atoms cm^3. At 1000 K, the interdiffusion diffusion coefficient of lithium in nickel is 5×10^{-8} cm s^{-1}.

13.21 A cylindrical bar of Fe (dia. of 1 cm) is suspended in a well mixed and small melt of Mn maintained at 1300°C. Assume that there is local equilibrium at the solid-liquid interface and calculate the time required to raise the manganese composition at the center of the bar to 1 wt.%. The interdiffusion coefficient of Mn in Fe is given by

$$D = 0.49 \exp\left[-\frac{33\ 200}{T}\right]$$

with T in K and D in $cm^2\ s^{-1}$.

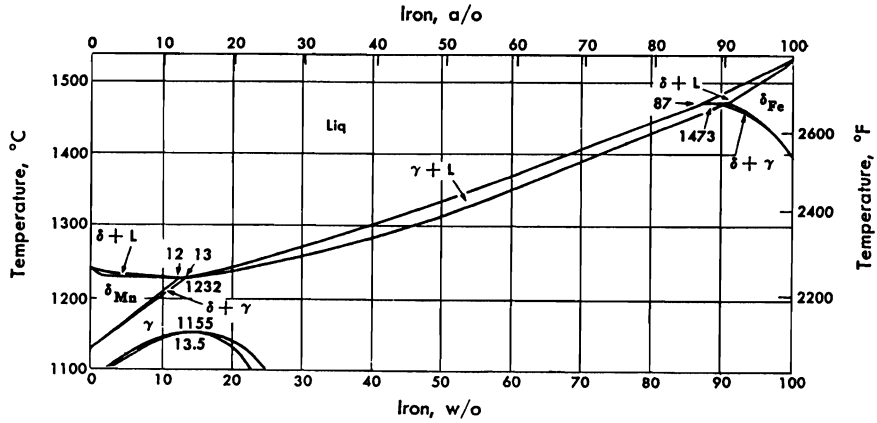

13.22 A very thin sheet of Fe-0.2 atom fraction B is "sandwiched" between two large pieces of iron, and then the entire assembly is heated to 1000°C. The sheet is only 5×10^{-3} cm thick and at 1000°C diffusion bonding occurs as the boron diffuses into the iron. Assume that the boron is completely soluble and that there is only a single phase. a) Calculate the time required for the concentration of B to achieve its maximum at a distance of 1 mm from the original joint. b) What is the maximum concentration at 1 mm? c) At the time corresponding to part a), what is the atom fraction of B at the original joint?

13.23 A batch of steel exhibits "banding," which is a form of microsegregation in the wrought condition. The spacing between the bands is 50 μm. After 10 h of a high temperature homogenization treatment, the residual segregation index is 0.2 (determined by electron beam microanalysis). A second batch of the same type of steel has a band spacing of 100 μm. How long must this batch be maintained at the high temperature to achieve the same residual segregation index of 0.2?

13.24 A melt with uniform concentration of solute, C_∞, is solidified with a planar interface. Chemical equilibrium is maintained at the interface, which moves with a constant velocity V. The concentration profile at steady state, with no convection in the liquid, is as depicted:

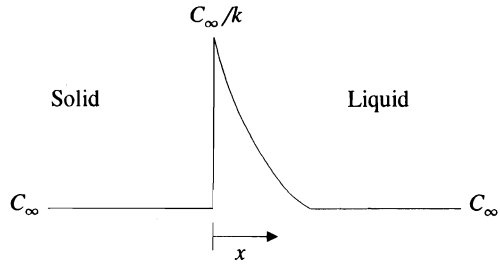

a) Use a moving coordinate system with the origin ($x = 0$) at the solid-liquid interface and derive the differential equation for the concentration profile in the liquid.
b) Write appropriate boundary conditions and solve for $C(x)$.
c) Determine the concentration gradient in the liquid at $x = 0$. How does the concentration gradient relate to the velocity of the interface?
d) The characteristic length, δ, defined by

$$j_0 = \frac{D}{\delta}\left[\frac{C_\infty}{k} - C_\infty\right],$$

where j_0 is the diffusional flux at the interface ($x = 0$). Determine δ in terms of the solidification velocity and the concentration gradient at the interface.

13.25 A powder-ceramic compact is outgassed at 500°C in a chamber filled with pure argon in order to remove air before sintering. The tortuosity of the compact is 4, its porosity is 0.2, and the average pore radius is 200 Å. The compacts are 50 mm long × 25 mm diameter. Calculate the fraction of air remaining after 1 h of outgassing treatment.

13.26 In order to make a transformer steel with the proper hysteresis loop, a low silicon steel sheet (2 mm thick) is to be exposed on both sides to an atmosphere of $SiCl_4$ which dissociates to Si(g) and Cl_2(g). The Si(g) dissolves in the steel up to 3 wt.% at equilibrium. a) Indicate what partial differential equation and what boundary and initial conditions would apply in order to calculate the diffusion of Si into the sheet. b) Using the data in Fig. 12.11, calculate the time to achieve an average concentration of 2.85 wt.% Si at 1255 K.